Institute of Nuclear Physics

N.S. Dikansky, V.I. Kudelainen, V.A. Lebedev,
I.N. Meshkov, V.V. Parkhomchuk, A.A. Sery,
A.N. Skrinsky, B.N. Sukhina

ULTIMATE POSSIBILITIES OF ELECTRON COOLING

PREPRINT 88-61

NOVOSIBIRSK
1988

Ultimate Possibilities of Electron Cooling

N.S. Dikansky, V.I. Kudelainen, V.A. Lebedev,
I.N. Meshkov, V.V. Parkhomchuk, A.A. Sery,
A.N. Skrinsky, B.N. Sukhina

Institute of Nuclear Physics
630090, Novosibirsk 90, USSR

ABSTRACT

Review of experimental results on electron cooling studing in the range of small relative velocities on NAP-M and «Model of Solenoid» devices at 1976—1988 is presented.

1. INTRODUCTION

The method of electron cooling proposed by G.I. Budker in 1966 [1] has been developed in experimental and theoretical studies in Novosibirsk [2], which resulted in the discovery of fast electron cooling [3—6]. The experiments carried out first in Novosibirsk and some time later at CERN [7] and Fermilab [8] proved the possibility of deep cooling of beams of heavy particles circulating in the storage ring. The possibilities of electron cooling were further studied in Novosibirsk on the installation «Solenoid model» [9, 10]. The maximum friction force obtained in these experiments is by the order of magnitude higher than that obtained earlier in Novosibirsk on the NAP-M installation [6]. This value is close to the theoretical limit determined by the density of electrons $F_{max} \sim e^2 n^{2/3}$. At present the results obtained enable to make the more complete formulation of the regularities in behaviour of the friction force at the electron cooling in the region of low relative velocities of ions under conditions of magnetized electron flux.

The present status of the electron cooling technique enables one to work with the supercooled beams of heavy particles whose temperature in an accompanying reference system is $\leqslant 1$K. It opens up the new in principle possibilities for experiments in atomic and nuclear physics. For antiproton storage the electron cooling, if combined with the stochastic one, actually removes limitations for obtaining cooled antiproton beams of high intensity. The development of the method of electron cooling [11] resulted in the appearance of a new direction in the acceleration physics, namely the physics of ultracooled beams which is at present under active development in a number of laboratories in the world.

2. INTERACTION PICTURE

The electron cooling method is based on the heat exchange between the beam of charged heavy particles (in future named ions) circulating in the storage ring, and the beam of electrons having the same average velocity [1]. At low relative ion velocities the friction force, that appears due to the Coulomb interaction with electron, increases sharply which permits obtaining sufficiently short cooling times at attainable electron densities. The cooling time corresponds to the time of temperature relaxation of the ion gas in the electron flux. As a result, the phase volume of the heavy particle beam reduces over all the degrees of freedom. This reduction continues till the temperature of the heavy particle gas reaches the effective electron temperature.

The kinetics of electron cooling has a number of peculiarities that differs it from the common relaxation of a two-component plasma. These peculiarities are due to the strong anisotropy of the function of electron distribution over velocities, due to the strong magnetic field accompanying the electron beam, as well as to the finite time of the ions' interaction with the electron beam. In calculations the nonrelativistic approximation is used which can be easily extended to a relativistic case.

2.1. Electron Distribution Function over Velocities

In the electron cooling installation the beam of electrons is generated in the gun placed in the magnetic field to prevent an electrostatic scattering of electrons in the cooling section [2]. In the process of study of electron cooling it was discovered that in this case, after the electrostatic accelaration of the electron beam the longitudinal temperature in an accompanying reference system will be much lower than the transversal one [3]. In first approximation one can take that the flux of electrons from the cathode surface is described by the Maxwell distribution of electrons over velocities:

$$dj(v_{\parallel}, v_{\perp}) = j_c \frac{m^2}{T_c^2} \exp\left[-\frac{m}{2T_c}(v_{\perp}^2 + v_{\parallel}^2)\right] v_{\perp}\, dv_{\perp} v_{\parallel}\, dv_{\parallel} \qquad (2.1)$$

where j_c, T_c—are the saturation current density and the cathode temperature respectively. If the electron-electron interaction is negligibly small and the electron gun has sufficiently good optics the distribution function over transverse velocities is not changing with acceleration and the transverse temperature of electrons $T_{\perp}$ remains equal to the cathode temperature ($T_{\perp} = T_c$). It is convenient to estimate the longitudinal temperature using the distribution function of electrons over the longitudinal energy:

$$dj = j_c e^{-\mathscr{E}/T_c} \frac{d\mathscr{E}}{T_c}, \qquad \mathscr{E} = \frac{mv_{\parallel}^2}{2}. \qquad (2.2)$$

During acceleration the energy $\mathscr{E}$ acquires an increment eU_c, where U_c is accelerating potential difference. If the gun operates in the regime of the limitation of the current density j by the space charge of the electron beam («regime 3/2»), then the minimum of potential $U_{\min} = -\frac{T_c}{e} \ln \frac{j_c}{j}$ is generated near the cathode, reflecting an superfluous current from the cathode. The presence of the potential minimum results in an increase of the average electron energy in the beam $\bar{\mathscr{E}}_e$ by the value $U_{\min}$. By replacing $\mathscr{E} \to \mathscr{E} + eU_c + T_c \ln(j_c/j)$ in (2.2) and averaging it over energy we obtain an average energy for electrons in the beam

$$\bar{\mathscr{E}}_e = eU_c + T_c(1 + \ln(j_c/j)). \qquad (2.3)$$

Though the distribution function (2.2) is not thermodynamically equilibrium one, we can introduce an effective longitudinal temperature in an accompanying reference system:

$$T_{\parallel} = \langle m \Delta v_{\parallel}^2 \rangle = \frac{T_c^2}{2W}, \qquad W = eU_c. \qquad (2.4)$$

From expression (2.4) it is evident that longitudinal temperature of electrons in the accelerated beam is much lower than the transverse one (being equal to T_c) and decreases rapidly with an increase in the energy of electrons.

As a rule, under real experimental conditions the noninteracting electrons approximation is not valid and one should take into account the internal interaction (collisions) of electrons in the beam leading to an increase in the longitudinal temperature of electrons.

When transporting an electron beam its longitudinal temperature increases due to the internal scattering of electrons with the energy transfer of the transverse motion into the longitudinal one. Such a relaxation of temperature (transverse-longitudinal relaxation) accurs untill having the equilibrium in the longitudinal and the transversal temperatures. If one can neglect the influence of the magnetic field at $T_{\parallel} \ll T_{\perp}$ the relaxation can easily be calculated [12]:

$$\frac{dT_{\parallel}}{dz} = \frac{\pi e^3 j L_C k}{W} \sqrt{\frac{m}{T_{\perp}}} \tag{2.5}$$

where $z = v_0 t$ is a longitudinal coordinate, L_C is a Coulomb logarithm, k is a numerical coefficient depending on the kind of the distribution function of electrons over transverse velocities (for the Maxwell distribution $k \simeq 0.87$). An increase in the longitudinal temperature (2.5) goes quite rapidly, so at $W = 450$ eV, $j = 0.5$ A/cm^2 both the temperatures become equal at a distance of 3 m. Note, that in this case, the electron energy spread in the laboratory system is $\delta\mathscr{E} \simeq \sqrt{2WT_c} \simeq 10$ eV (when $T_c = 0.1$ eV).

The strong magnetic field changes substantially the kinetics of electron collisions. If its intensity is sufficiently large, an average Larmour radius of the electron transverse rotation is much lower than the distance between them:

$$\rho_{\perp} \ll n^{-1/3} \tag{2.6}$$

where n is the density of electrons. In this case, if the longitudinal temperature of electrons is sufficiently small the electron collisions are of an adiabatic character and the energy transfer from the transverse motion into the longitudinal one is suppressed. The estimation of the longitudinal temperature follows from the condition of smallness of the Larmour radius of electron rotation compared to the distance of the minimal probable distance between electron $r_{\min} \sim e^2/T_{\parallel}$:

$$T_{\parallel} \ll e^2/\rho_{\perp}. \tag{2.7}$$

The use of inequalities (2.6), (2.7) defines the conditions for suppression of the transverse-longitudinal relaxation. At $T_{\perp} = 0.1$ eV, $n = 10^9$ cм$^{-3}$, we get $B \gg 1$ kG, $T_{\parallel} \lesssim 10^{-4}$ eV.

Another effect leading to an increase in the longitudinal beam temperature is the longitudinal-longitudinal relaxation. In an ordinary electron gun the acceleration of electrons proceeds quickly compared to the period of plasma oscillation of electrons. Therefore, for the time of acceleration the disposition of electrons does not practically change and its initial state with the chaotic disposition of electrons («Larmour circles») in the beam is preserved. Since the longitudinal temperature is small after acceleration: $T_{\parallel} \simeq T_c^2/2W$, the absence of correlations in positions of electrons leads (due to the electrostatic repulsion) to its increase by the value $\sim e^2 n^{1/3}$. As a result we get the value of longitudinal temperature

$$T_{\parallel} \simeq \frac{T_c^2}{2W} + Ce^2 n^{1/3}. \tag{2.8}$$

The value of constant $C \simeq 2$ will be calculated below (see s. 4.1) The time of such a relaxation is small and by the order of magnitude equals to the period of plasma oscillations. In this time an electron passes the distance of the order of a few distances between the cathode and the anode. In contrast to the transverse-longitudinal relaxation such a relaxation is not suppressed by the magnetic field. Usually, the second in (2.8) is much higher than the first one and namely this fact determines the longitudinal temperature:

$$T_{\parallel} \simeq 2e^2 n^{1/3} \simeq 3 \cdot 10^{-4} \text{ eV}$$

at $n = 10^9$ cм$^{-3}$.

To obtain the value of temperature lower than $e^2 n^{1/3}$ one can use a slow (if compared to the period of plasma oscillation) acceleration of electrons in the gun. In this case the plasma oscillations are flattening the density fluctuations for the time of acceleration and the longitudinal temperature can be lower than $e^2 n^{1/3}$ (see below, s. 4.1)

2.2. Friction Force in the Absence of Magnetic Field

In the absence of the magnetic field the friction force affecting on the ion travelling in an electron gas with the distribution function ove velocities $f(\mathbf{v})$ is expressed by the well known formula [1]:

$$\mathbf{F} = -\frac{4\pi n e^4 Z^2 L_C}{m} \int \frac{\mathbf{v}_p - \mathbf{v}}{|\mathbf{v}_p - \mathbf{v}|^3} f(\mathbf{v})\, d^3 v \tag{2.9}$$

where Ze, $\mathbf{v}_p$ are the charge and the velocity of ion, m is the electron mass, n is the electron density, $f(\mathbf{v})$ is normalized to unit magnitude, L_C is the Coulomb logarithm:

$$L_C = \ln \frac{\rho_{max}}{\rho_{min}}, \quad \rho_{max} \simeq \min\left\{ \frac{\langle |\mathbf{v}_p - \mathbf{v}_e| \rangle}{\omega_{pe}}, \tau \langle |\mathbf{v}_p - \mathbf{v}_e| \rangle, a \right\},$$

$$\rho_{max} \gg \rho_{min}, \quad \rho_{min} = \frac{Ze^2}{m\langle |\mathbf{v}_p - \mathbf{v}_e| \rangle^2}, \quad \omega_{pe} = \sqrt{\frac{4\pi n e^2}{m}} \qquad (2.10)$$

where τ is the ion time in the electron beam, a is the electron beam radius.

Let the distribution function have the quasi-Maxwell form

$$f(v_\parallel, v_\perp) = \frac{m^{3/2}}{(2\pi)^{3/2} T_\perp T_\parallel^{1/2}} \exp\left(-\frac{mv_\parallel^2}{2T_\parallel} - \frac{mv_\perp^2}{2T_\perp}\right), \quad T_\parallel \ll T_\perp, \qquad (2.11)$$

that takes into account the flatness of electron distribution function along the direction of the electron beam velocity. By integrating (2.9) with an account of (2.11) for the friction force (in the particles system) with the ion travelling in the direction of the beam motion we get:

$$F_\parallel(v_{p\parallel}) = -\frac{4\pi n e^4 Z^2 L_C}{m} \begin{cases} 1/v_{p\parallel}^2, & |v_{p\parallel}| > v_{e\perp}, \\ 1/v_{e\perp}^2, & v_{e\perp} \gg |v_{p\parallel}| \gg v_{e\parallel}, \\ v_{p\parallel}/((2\pi)^{3/2} v_{e\perp}^2 v_{e\parallel}), & |v_{p\parallel}| \ll v_{e\parallel}. \end{cases} \qquad (2.12)$$

Similarly, when travelling in the transverse direction

$$F_\perp(v_{p\perp}) = -\frac{4\pi n e^4 Z^2 L_C}{m} \begin{cases} \dfrac{1}{v_{p\perp}^2}, & v_{p\perp} \gg v_{e\perp}, \\ \sqrt{\dfrac{\pi}{8}} \dfrac{v_{p\perp}}{v_{e\perp}^3}, & v_{p\perp} \ll v_{e\perp}. \end{cases} \qquad (2.13)$$

Here

$$v_{e\perp} = \sqrt{\frac{T_\perp}{m}}, \quad v_{e\parallel} = \sqrt{\frac{T_\parallel}{m}} \qquad (2.14)$$

is the heat spread of electrons' velocities. In the region of intermediate values of the ion velocities the friction force was calculated by the numerical integration with the results being presented in Fig. 1.

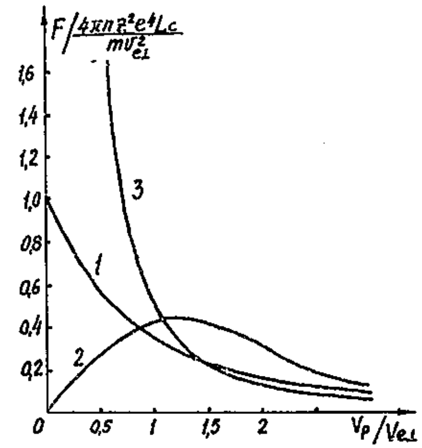

Fig. 1. The longitudinal (curve *1*) and transversal (curve *2*) friction force as a function of the ion (proton) velocity obtained by the numerical integration of expressed (2.9) for the quasi-Maxwell distribution function (2.11). Curve. *3* is the dipendence of the transversal friction force on the ion velocity in the case of «magnetized» collisions of electrons with the ion (in accordance with (2.16), $v_{p\parallel}=0$).

From the expressions obtained it is evident that at $v_p > v_{e\perp}$ the friction force decreases proportionally v_p^{-2}, and the friction force maximum is determined by the transverse temperature of electrons:

$$F_{max} \simeq \frac{4\pi n e^4 Z^2 L_C}{m v_{e\perp}^2} = \frac{4\pi n e^4 Z^2 L_C}{T_\perp}. \qquad (2.15)$$

2.3. Friction Force in the Ultimately Magnetized Flux of Electrons

The magnetic field limits the transversal motion of electrons. If the magnetic field is sufficiently strong the collisions between electrons and the ion become adiabatic with respect to the Larmour rotation of electrons at sufficiently large impact parameters. In this case, electrons (the Larmour circles) can travel only along the field and the transverse degree of freedom of electrons is excluded from the kinetics of collisions. Therefore, the electron cooling efficiency is determined by the longitudinal temperature of electrons that is by a few orders of magnitude lower than the transverse one. A decrease in the effective temperature leads to the further increase of the friction force with lowering the ion velocity in the region $v_p < v_{e\perp}$. This growth of the friction force $\sim 1/v_p^2$ continues until the ion velocity decreases down to the level $v_p \simeq v_{e\parallel}$ (Fig. 1, curve *3*). The maximum value of the friction force in this case is by a few orders of magnitude larger than that in the case of nonmagnetized collisions [4].

The expressions for the friction force in the ultimately magnetized electron flux when electrons can travel only along the magnetic field were first obtained in Ref. [4]. In case when the heat spread of the electron velocities is small if compared to the ion velocity the friction force components along ($F_{\parallel}$) and transverse ($F_{\perp}$) to the magnetic field will be equal to

$$F_{\parallel} = -\frac{2\pi n e^4 Z^2 L_C}{m v_p^2} \frac{3 v_{p\parallel} v_{p\perp}^2}{v_p^3},$$

$$F_{\perp} = -\frac{2\pi n e^4 Z^2 L_C}{m v_p^2} \frac{v_{p\perp}(v_{p\perp}^2 - 2 v_{p\parallel}^2)}{v_p^3} \qquad (2.16)$$

where $v_{p\parallel}$, $v_{p\perp}$ are the longitudinal and the transverse (with respect to the magnetic field) components of the ion velocity. v_p, L_C is the Coulomb logarithm determined by expression (2.10). From (2.16) it is easy to get the components of the friction force along ($\mathscr{F}_{\parallel}$) and transverse ($\mathscr{F}_{\perp}$) to the ion velocity:

$$\mathscr{F}_{\parallel} = -\frac{2\pi n e^4 Z^2 L_C}{m v_p^2} \frac{v_{p\perp}^2}{v_p^2},$$

$$\mathscr{F}_{\perp} = \frac{2\pi n e^4 Z^2 L_C}{m v_p^2} \frac{2 v_{p\parallel} v_{p\perp}}{v_p^2}. \qquad (2.17)$$

In Ref. [11] the expressions were obtained for the friction force differing from (2.17) by a twice lower value of the friction force $\mathscr{F}_{\perp}$, transverse to the ion velocity. In Appendices the calculations of the friction force for both the ways are given. Below we shall discuss the reasons of difference in results and carry out more accurate calculations of the friction force in case of the ultimate magnetization.

The first way of calculation [4] is based on an account of the collective reaction of the electron plasma. The electric field of a travelling ion leads to perturbation of density in the electron plasma and consequently to the excitation of the electric field. The electric field value (produced by electrons) in the point of the ion disposition determines the friction force value. In order to find out the electric field let us linearize the Vlasov equation for the electron distribution function over velocities:

$$\frac{\partial f}{\partial t} + v_z \frac{\partial f}{\partial z} - \frac{e}{m} E_z \frac{\partial f_0}{\partial v_z} = 0 \qquad (2.18)$$

and solve it together with the Poisson equation

$$\operatorname{div} \mathbf{E} = 4\pi\left(-e\int f\, dv + Ze\delta(\mathbf{r} - \mathbf{v}_p t)\right). \qquad (2.19)$$

It is accepted here that the magnetic field is directed along axis z, the ion travels with a constant velocity $\mathbf{v}_p$, electrons are magnetized and can travel only along the magnetic field that leads to elimination of derivations over x, y in equation (2.18). Since the spread of the longitudinal velocities of electrons is very small, then without limiting the generality one can assume that the ion velocity is large compared to the electrons energy spread $v_p \gg v_{e\parallel} = \sqrt{e^2 n^{1/3}/m}$. This condition coincides with the condition of applicability of the logarithmic approximation (2.10). By performing the Fourier transformation over time and coordinates and substituting (2.18) in (2.19) we have

$$\mathbf{E}_{k\omega} = \frac{4\pi \mathbf{k}}{ik^2} \frac{\rho_{k\omega}}{\varepsilon(\mathbf{k}, \omega)}, \qquad \rho_{k\omega} = 2\pi e Z \delta(\omega - (\mathbf{k}, \mathbf{v}_p)), \qquad (2.20)$$

$$\varepsilon(\mathbf{k}, \omega) = 1 + \frac{4\pi e^2 k_z}{m k^2} \int \frac{\partial f_0}{\partial v_z} \frac{d^3 v}{\omega - (\mathbf{k}, \mathbf{v}_p)} \qquad (2.21)$$

At $v_p \gg v_{e\parallel}$ the result can easily be obtained by the integration by parts

$$\varepsilon(\mathbf{k}, \omega) = 1 - \frac{4\pi n e^2}{m\omega^2} \frac{k_z^2}{k^2} + \frac{i\delta}{\omega}, \qquad \delta \ll \omega_{pe} \equiv \sqrt{\frac{4\pi n e^2}{m}}. \qquad (2.22)$$

The imaginary part of the dielectric penetration appears while passing around the pole $\omega = (\mathbf{k}, \mathbf{v}_p)$. The Fourier reverse transformation gives the electric field in a plasma:

$$\mathbf{E}(\mathbf{r}, t) = \frac{eZ}{2\pi^2 i} \int \frac{\mathbf{k}}{k^2} \frac{d^3 k\, d\omega}{\varepsilon(\mathbf{k}, \omega)} e^{-i(\omega t - \mathbf{k}\mathbf{r})} \delta(\omega - (\mathbf{k}, \mathbf{v}_p)) \qquad (2.23)$$

and the friction force affecting on the ion:

$$\mathbf{F}_{fr} = Ze\mathbf{E}(\mathbf{v}_p t, t) = \frac{Z^2 e^2}{2\pi^2} \int_0^{k_{max}} \frac{\mathbf{k}}{k^2} d^3 k \,\operatorname{Im}\left(\frac{1}{\varepsilon(\mathbf{k}, (\mathbf{k}\mathbf{v}_p))}\right). \qquad (2.24)$$

By calculating the integral (see Appendix 1) we obtain expression (2.17) for the friction force. While calculating the integral to eliminate the logarithmic divergence at $k \to \infty$ one should limit the integration region by the value k_{max}. This is connected with the violation of the conditions of applicability of the perturbation theory for small distances. The minimal impact parameter $1/k_{max}$ is defined by the condition of a small value for the density perturbation of the electron plasma. After the ion passage the region behind it remains free of electrons that then disappears in the time of plasma oscillations $\tau\sim\omega_{pe}^{-1}$. The dimensions of this region in the directions both along and transverse to the ion motion are equal to:

$$r_{\parallel}\simeq v_p/\omega_p\,,\qquad r_{\perp}\simeq\frac{e^2Z}{mv_\rho r_{\perp}}\,\frac{1}{\omega_p},\qquad \text{or}\qquad r_{\parallel}\simeq\rho_{max}\,,\qquad r_{\perp}\simeq\sqrt{\rho_{max}\rho_{min}}\,, \tag{2.25}$$

and its volume is of the order of n^{-1}.

Thus, the considered method for solving the problem by finding out the perturbation of the electron distribution function enables one to take correctly into account the contribution of collisions with large impact parameters, takes into account the shielding of the Coulomb interaction at $\rho>\rho_{max}$, but it is violated at values of the impact parameters $\rho\lessapprox\sqrt{\rho_{max}\rho_{min}}$ exceeding substantially the minimal impact parameter ρ_{min}. In addition, the cut of the integration upper limit at $k=k_{max}$ does not exclude the collisions with small impact parameters, but just modifies the Coulomb potential of the interacting ion:

$$\varphi=\frac{Ze}{r}\to\varphi=-\frac{Ze}{2\pi^2}\int\limits_0^{k_{max}}\frac{d^3k}{k^2}e^{i(\mathbf{k},\mathbf{r})}=$$

$$=\frac{2}{\pi}\,\frac{Ze}{r}\int\limits_0^{rk_{max}}\frac{\sin x}{x}\,dx=\frac{Ze}{r}\frac{2}{\pi}\,\mathrm{Si}(k_{max}r)\,. \tag{2.26}$$

Therefore, before to turn to the correct account of contributions to the friction force of collisions with low impact parameters one needs to subtract from the expressions obtained the contributions to the friction force made by the collisions with impact parameters $\rho<1/k_{max}\ll\rho_{max}$.

Within the logarithmic accuracy one can take that an interaction between an electron and ions occurs instantaneously at $r=\rho_{max}$. Then an electron shift along the magnetic field to the moment

of the minimal distance between an ion and an electron is (see Appendix 2)

$$\xi=\frac{Ze}{mv^2}\left[\sin\theta\,\cos\varphi+\cos\theta\left(\ln\,\frac{2\rho_{max}}{\rho}-1\right)\right]\to\frac{Ze^2}{mv^2}\,\cos\theta\,\ln(k_{max}\rho_{max}) \tag{2.27}$$

where θ is an angle between the ion velocity and the magnetic field. The maximum value of ξ is achieved at the value of the impact parameter equal to the radius at which the Coulomb potential is cut $\rho=1/k_{max}$. The shift of electrons along the field leads to the transverse shift, as a whole, of a cylinder containing electrons with impact parameters $\rho<=k_{max}^{-1}$ by the value $\Delta=\xi\sin\theta$. This shift results in occuring the transverse electric field acting on the ion and consequently to the appearance of the friction force transverse to the velocity:

$$\mathscr{F}_{\perp}=ZeE_e=Ze\cdot 2\pi ne\xi\sin\theta=\frac{2\pi ne^4Z^2}{mv^2}\ln(k_{max}\rho_{max})\sin\theta\cos\theta\,. \tag{2.28}$$

It is easy to check that differing from the transverse friction force the collisions with low impact parameters do not give the logarithmic contribution into the longitudinal friction force and the variation of longitudinal friction force due to these collisions can be neglected. From (2.17) by subtracting the contribution of collisions with low impact parameters (2.28) we obtain a twice lower value of the transverse component of the friction force (transverse with respect to the ion velocity) that in accordance that is in accordance with the results of Ref. [11].

The consideration performed takes into account the contribution into the friction force given by collisions with impact parameters

$$\rho_{max}>\rho>r_{\perp}\cong\sqrt{\rho_{max}\rho_{min}} \tag{2.29}$$

which give approximately a half of the friction force value. For impact parameters

$$\sqrt{\rho_{max}\rho_{min}}>\rho>\rho_{min}\ln\frac{\rho_{max}}{\rho_{min}} \tag{2.30}$$

the collisions can be taken as single-particle ones. Their contribution into the friction force (see Appendix 2) is the same as the contribution of collisions with high impact parameters. As a result we have

$$\begin{pmatrix} \mathscr{F}_{\parallel} \\ \mathscr{F}_{\perp} \end{pmatrix} = -\frac{2\pi n e^4 Z^2 L_C}{m v_p^2} \begin{pmatrix} v_{p\perp}^2/v_p^2 \\ -v_{p\parallel} v_{p\perp}/v_p^2 \end{pmatrix}, \qquad (2.31)$$

$$L_C \simeq \ln\left(\frac{\rho_{max}}{\sqrt{\rho_{max}\rho_{min}}}\right) + \ln\left(\frac{\sqrt{\rho_{max}\rho_{min}}}{\rho_{min}\ln\left(\frac{\rho_{max}}{\rho_{min}}\right)}\right) \simeq \ln\left(\frac{\rho_{max}}{\rho_{min}}\right).$$

For obtaining the final result one should add to this expression the contribution into the friction force given by low impact parameters.

Differing from the nonmagnetized collisions in the case of strong magnetization the contribution into the friction force given by collisions with low impact parameters $\rho \lesssim \rho_{min} \ln(\rho_{max}/\rho_{min})$ is not small compared to the logarithm and depends of the charge sign of the colliding ion. This becomes of special importance when the ion velocity is low and the Coulomb logarithm differs slightly from the unit. So, the negatively charged ion while travvelling along the magnetic field pushes forward electrons located at an impact distance $\rho < \rho_{min}$. In this case, the electron momentum changes by $2mv_p$. In the case of a positively charged ion such electrons will pass near ion without changes in its momentum. As a result, an additional contribution into the friction force for negatively charged ions appears:

$$\Delta F_{\parallel} = -\pi \rho_{min}^2 \cdot 2mv_p \cdot nv_p = -\frac{8\pi n e^4 Z^2}{m v_p^2}. \qquad (2.32)$$

In addition, in a strong magnetic field the collisions with low impact parameters both for positively and negatively charged ions (corresponding to (2.28)) can give a logarithmic contribution into the friction force transverse to the ion's velocity.

So, the equations of electron motion in the field of colliding ion is not integrable, the contribution of low impact parameters into the friction force was calculated by computer simulation in the single-particle approximation. The electron field of ion started instantaneously at $r = \rho_{max}$. The contribution to the friction force versus impact parameter obtained by computer simulation is shown on Fig. 2. The friction force was defined by the function $f(\rho)$, (given in the Figure) with the integration over the impact parameter:

$$\mathscr{F}_{\parallel,\perp} = \frac{2\pi n e^4 Z^2}{m v_p^2} \int_0^{\rho_{max}} f_{\parallel,\perp}(\rho) \frac{d\rho}{\rho}. \qquad (2.33)$$

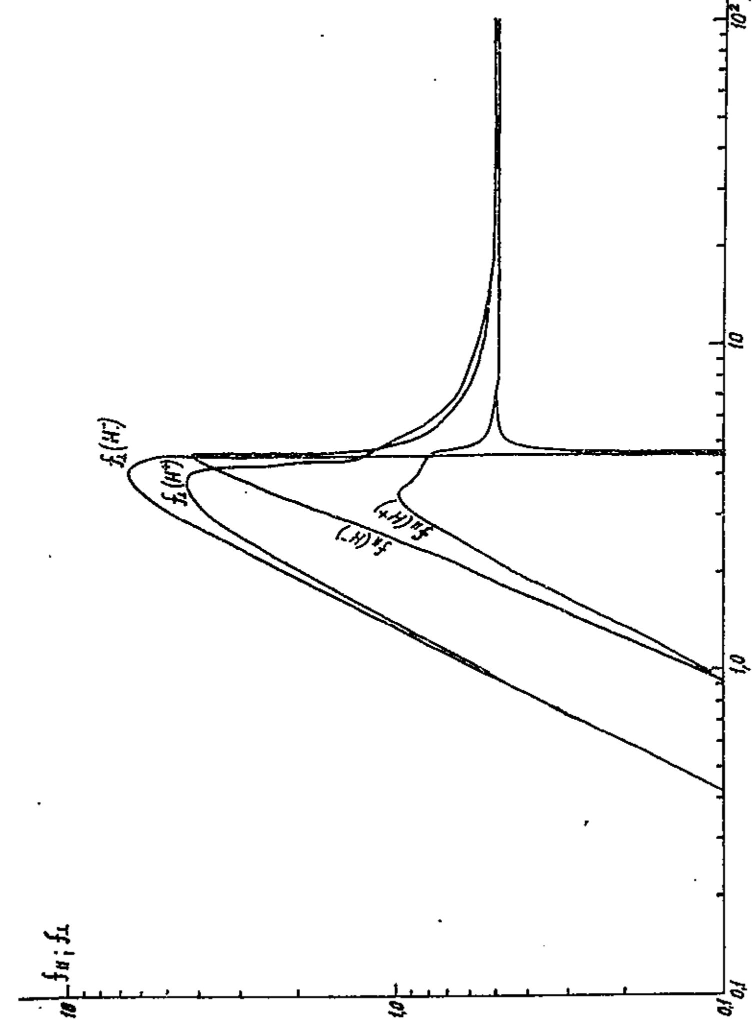

Fig. 2. Relative contribution into longitudinal and transverse components of friction force $f_{\parallel,\perp}$ of various impact parameters for positively and negatively charged ions. The angle between ion velocity and magnetic field is $\theta = 45°$, $\rho_{max}/\rho_{min} = 10^4$.

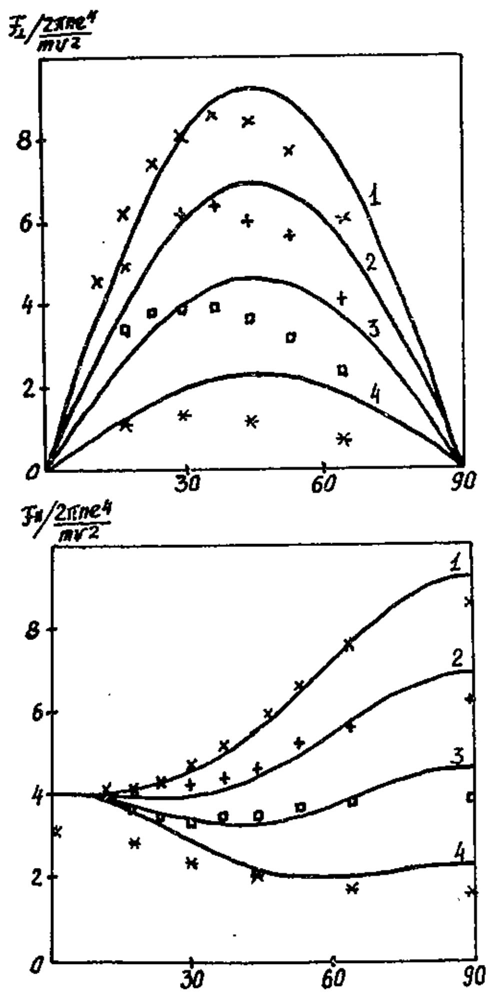

Fig. 3. Longitudinal and transverse (with respect to velocity) components of friction force for negatively charged ion as a function of an angle between the velocity and magnetic field for various relations $\frac{\rho_{max}}{\rho_{min}}$ (ion various velocities $\frac{\rho_{max}}{\rho_{min}} = \frac{m^{3/2} v_p^3}{\sqrt{4\pi n}\, z e^3}$).

ρ_{max}/ρ_{min}	10^4	10^3	10^2	10
function (2.34)	*1*	*2*	*3*	*4*
numerical calculation	×	+	□	*

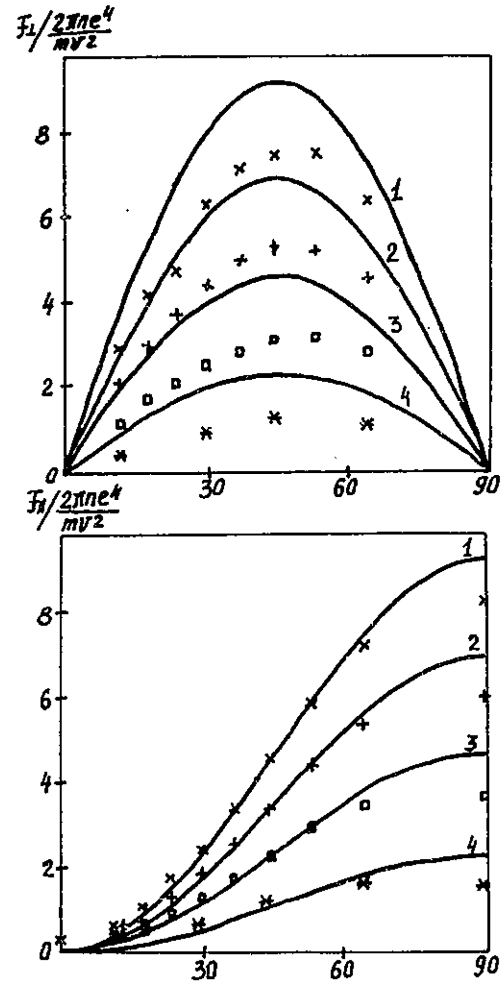

Fig. 4. Longitudinal and transverse (with respect to velocity) components of friction force for positively charged ion as a function of an angle between the velocity and magnetic field for various relations $\frac{\rho_{max}}{\rho_{min}}$, (ion various velocities: $\frac{\rho_{max}}{\rho_{min}} = \frac{m^{3/2} v_p^3}{\sqrt{4\pi n}\, Z e^3}$).

ρ_{max}/ρ_{min}	10^4	10^3	10^2	10
function (2.34)	*1*	*2*	*3*	*4*
numerical calculation	×	+	□	*

As it is seen from the Figure, at $\rho > \rho_{min} \ln(\rho_{max}/\rho_{min})$ the relative contribution given by various impact parameters does not depend on ρ and coincides with the results of the calculations carried out according to the perturbation theory (see Appendix 2). At low impact parameters $\rho < \rho_{min} \ln(\rho_{max}/\rho_{min})$ the function $f_\perp$ increases both for positively and negatively charged ions. The numerical integration gives, that in the first approximation the contribution of low impact parameters into the longitudinal friction force is equal to the contribution of high impact parameters. The contribution of low impact parameters into the longitudinal friction force $\mathcal{F}_\parallel$ is only substantial for negative ions. This is due to the fact that the electron is pushed out along the magnetic field and it is essential at small angles between the ion velocity and the magnetic field. Figs. 3 and 4 show the longitudinal and transverse (with respect to the velocity) components of the friction force as functions of an angle θ between the ion velocity and the magnetic field. The curves given in Figs. 3 and 4 are drawn corresponding to the following expression

$$\begin{pmatrix} \mathcal{F}_\parallel \\ \mathcal{F}_\perp \end{pmatrix} = -\frac{2\pi n e^4 Z^2}{m v_p^2} \begin{pmatrix} L_C \sin^2\theta + 4\cos^4\theta\, \Theta(Z) \\ -2L_C \sin\theta \cos\theta \end{pmatrix}, \qquad (2.34)$$

$$\Theta(Z) = \begin{cases} 1, & Z<0, \\ 0, & Z>0, \end{cases}$$

that gives a satisfactory agreement with the results of numerical calculations. For the positively charged ions this result coincides with the result obtained in Ref. [4]. At $\rho_{max}/\rho_{min} = 10$ when the applicability conditions for the logarithmic approximation are already violated the results of the numerical simulation are closer to the expression suggested in Ref. [11].

2.4. Friction Force in Magnetic Field of Finite Intensity

In a magnetic field of finite intensity the adiabaticity condition for collisions can be violated at low impact parameters. The minimal impact parameter of adiabatic collisions is defined by following expression: $\rho_{ad} > v_p \Omega_e^{-1}$, $\rho_\perp$ so, that:

$$\rho_{ad} = \max\left(\frac{2e^2}{m v_p}, \rho_\perp, \frac{v_p}{\Omega_e}\right) \qquad (2.35)$$

where $\rho_\perp$, Ω_e are the radius and frequency of Larmour motion of electrons.

If the ion velocity is high compared to an average transverse velocity of electrons $v > v_{e\perp}$, one can separate two characteristic regions of impact parameters: the region of high impact parameters $\rho_{max} > \rho > \rho_{ad}$, where collisions between an ion and an electron are adiabatic and the region of low impact parameters $\rho_{ad} > \rho > \rho_{min}$, where the magnetic field influence on the collisions can be neglected. In this case, the friction force is equal to

$$F_\perp = -\frac{2\pi n e^4}{m v^3} v_\perp \left(2L_{C1} + \frac{v_\perp^2 - 2v_\parallel^2}{v^2} L_{C2}\right),$$

$$F_\parallel = -\frac{2\pi n e^4}{m v^3} v_\parallel \left(2L_{C1} + \frac{3v_\perp^2}{v^2} L_{C2}\right), \qquad (2.36)$$

where the Coulomb logarithms of the fast and adiabatic collisions are respectively:

$$L_{C1} = \ln\left(\frac{\rho_{ad}}{\rho_{min}}\right) = \ln\left(\frac{m^2 c v_p^3}{2e^3 B}\right),$$

$$L_{C2} = \ln\left(\frac{\rho_{max}}{\rho_{ad}}\right) = \frac{1}{2}\ln\left(\frac{B^2}{4\pi n m c^2}\right). \qquad (2.37)$$

Here it was taken into account that low impact parameters $\rho < \rho_{ad}$ make an additional contribution into the friction force component transverse to the ion velocity caused by the effect of the magnetic field (compare with (2.28)). The Coulomb logarithm of adiabatic collisions does not depend on the ion velocity and at a sufficiently strong magnetic field one cannot neglect the contribution made by adiabatic collisions even at high ion velocities $v_p \gg v_{e\perp}$. With a decrease in the ion velocity $v_p < v_{e\perp}$ the contribution of adiabatic collisions continues to grow proportionally to v_p^{-2}, while the contribution of fast collisions is limited by the transverse temperature of electrons (see (2.15)) and in the majority of cases it can be neglected.

If the condition $\rho_\perp < \rho_{max}$ is not satisfied, the contribution of adiabatic collisions turns to zero. Let us estimate the friction force in this case ($v_p \ll v_{e\perp}$, $\rho_\perp \gtrsim \rho_{max}$). Let the ion travel with the velocity v_p and collides with an electron having transverse velocity $v_{e\perp}$ ($v_{e\parallel} \ll v_{e\perp}$) and impact parameter ρ. The transfer of momentum to the electron for one collision is equal to

$$\Delta p_\perp \simeq \frac{2e^2 Z}{\rho v_{e\perp}}. \qquad (2.38)$$

In the case $\Omega_e(\rho/v_p)\gg 1$ the repeated electron-ion collision will take place and the total variation of the electron energy for the time of interaction ρ/v_p will be:

$$\Delta E=\frac{1}{2m}\left(\frac{2e^2Z}{\rho v_{e\perp}}\right)^2\frac{2\rho}{v_p}\,\frac{eB}{2\pi mc}. \qquad (2.39)$$

And we get estimate of the friction force:

$$F\simeq\int_0^{\rho_\perp}\Delta E\,2\pi\rho_\perp n d\rho=\frac{ne^4Z}{mv_pv_{e\perp}}\ln\left(\frac{\rho_{max}}{\rho_{min}}\right). \qquad (2.40)$$

In contrast to the case of ultimate magnetization ($\rho_\perp\ll\rho_{max}$) when with a decrease in v_p the friction force grows as v_p^{-2}, here the friction force grows only as v_p^{-1}. Such a dependence of the friction force on a velocity was observed in the experiments on NAP-M at $v_p<v_{e\perp}$ [5].

In all the previous estimates the condition of logarithmic approach applicability was considered as valid $\rho_{min}\ll\rho_{max}$. But in the process of cooling this condition is violated with a decrease in the ion velocity down to the value

$$v_p^*\simeq v_c\equiv\sqrt{\frac{2e^2n^{1/3}}{m}}. \qquad (2.41)$$

This velocity value corresponds to the characteristic spread of electron longitudinal velocities after a fast electrostatic acceleration (see (2.8)). Note, that an equilibrium value of the ion velocity is by $\sqrt{M/m}$ times less and therefore the logarithmic approach applicability condition is always violated close to equilibrium. The calculations in the velocity range $v\lesssim v_c$ are quite complicated. This is connected with the fact that the potential $e^2n^{1/3}$ and the kinetic $mv_{e\parallel}^2/2$ energies of the electron are of the same order and there is no low parameter over which one can use the perturbation theory. Therefore, let us confine ourselves by the simplest estimates that, as will be seen below, are in a good agreement with the experimental data. In the estimates we assume that $Z=\pm 1$. The friction force behaviour in the range of low velocities for multicharged ions requires an additional experimental study.

In order to obtain an estimate for the maximum value of the longitudinal friction force let us rewrite the expression (2.16) omitting an angular dependence:

$$F\simeq-\frac{2\pi ne^4}{mv_p^2}\ln\frac{\rho_{max}}{\rho_{min}}=-3\pi e^2n^{2/3}\frac{v_c^2}{v_p^2}\ln\left(\frac{v_p}{(2\pi)^{1/6}v_c}\right), \qquad (2.42)$$

$$v_c=\sqrt{\frac{2e^2n^{1/3}}{m}}.$$

By differentiating over v_p we get the velocity value at which the friction force attains its maximum value:

$$v_F\simeq(2\pi)^{1/6}e^{1/2}v_c\simeq 2.2\,v_c,\quad e=2.718\ldots \qquad (2.43)$$

and the maximum value of the friction force is

$$F_{max}^{+}\simeq 0.9e^2n^{2/3}. \qquad (2.44)$$

The expression obtained is valid for the positively charged ions (protons). For the negatively charged ions one has to take into account an addition to the friction force (2.32) determined by the collisions with low impact parameters:

$$F_{max}^{-}\simeq(0.9+2.5)e^2n^{2/3}=3.4e^2n^{2/3}. \qquad (2.45)$$

This addition leads to a significant difference in values of the longitudinal friction force for the positively and negatively charged ions. Though it makes a substantial contribution only in the range of low velocities when the Larmour radius of the electron rotation is small compared to the minimal impact parameter

$$\rho_\perp<\frac{2e^2}{mv^2}. \qquad (2.46)$$

Hence for the attainment of the friction force maximum value at $v=v_F$ it is necessary that

$$\rho_\perp\lesssim 0.2\,n^{1/3}. \qquad (2.47)$$

Assuming that at $v_p<v_c$ the friction force depends linearly on the ion velocity we get the cooling decrement value for the positively (negatively) charged ion at $v<v_c$:

$$\lambda_{max}^{\pm}\simeq 2\frac{F_{max}}{Mv_F}=\frac{m}{M}\sqrt{\frac{ne^2}{m}}\begin{cases}0.58, & z=1,\\ 2.2, & z=-1.\end{cases} \qquad (2.48)$$

From the estimations (see (2.43)) follows that the friction force attains its maximum value at the ion velocity exceeding the longitudinal electron velocity spread caused by their repulsion after acceleration $v_{e\parallel} \simeq \sqrt{2e^2 n^{1/3}/m}$ (see (2.8)). In the first approximation one can take that the friction force maximum value does not depend on the electron longitudinal temperature if $T_\parallel \leqslant 10e^2 n^{1/3}$.

Let us give a numerical example choosing the parameters typical for the electron cooling devices: $n = 10^9$ cm^{-3}, $T_\perp \simeq 0.1$ eV (an oxide thermocathode). Then we have:

$$T_\parallel = 2e^2 n^{1/3} \simeq 3\cdot 10^{-4} \text{ eV}, \quad v_F \simeq 10^6 \text{ cm/s},$$

$$F^+_{\max} = 0{,}13 \text{ eV/cm}, \quad F^-_{\max} = 0{,}5 \text{ eV/cm},$$

$$\lambda^+_{\max} = 1.6\cdot 10^5 \text{ s}^{-1}, \quad \lambda^-_{\max} = 6\cdot 10^5 \text{ s}^{-1},$$

$$B_0 > 5n^{1/3}\sqrt{2T_c mc^2}/e \simeq 5.3 \text{ kG}.$$

Here B_0 is a magnetic field necessary for attaining the maximum decrement while cooling negatively charged ions in correspondence with (2.47).

2.5. Equilibrium Values of Temperature

The difference in cooling of positively and negatively charged particles manifests itself not only in different values of the friction force but also in the substantially different values of diffusion of ions on electrons leading to the difference in the equilibrium values of temperature for the ions of different sign. Both the effective electron and the equilibrium ion temperatures are very small. In this case the plasma perturbation theory (logarithmic approximation) does not work and it becomes complicated to carry out both analytical and numerical calculations. Therefore, let us confine ourselves by simple estimates. In this case, the presence of additional «warming» factors will be neglected and the equilibrium temperature of ions is taken to be determined only the electron interaction in the process of cooling.

Let us first evaluate the diffusion coefficient for negatively charged ions while their travelling along the field. Near the equilibrium the ion velocity can be neglected compared to the electron velocity. The electron transverse motion can be taken as «frozen», and a longitudinal electron velocity is of the order of $v_c \equiv (2e^2 n^{1/3}/m)^{1/2}$. In this case the momentum transfer from electron to ion occurs only for the impact parameters less than $\rho_m \simeq \min(2e^2/mv^2_{e\parallel}, n^{-1/3}/2) = n^{-1/3}/2$, and it is equal to $2mv_c$. Then the diffusion

coefficient is

$$\frac{d}{dt}\langle \Delta p^2_{a\parallel}\rangle \simeq \pi\rho^2_m n v_c (2mv_c)^2 = \frac{4\pi n e^4}{v_c}, \tag{2.49}$$

and an equilibrium temperature for negative ions is of the order of

$$T^-_\parallel \simeq \frac{1}{2M\lambda^-}\frac{d}{dt}\langle \Delta p^2_{a\parallel}\rangle \simeq 2e^2 n^{1/3}. \tag{2.50}$$

A similar evaluation can be done for the transverse temperature and one can find out that it is of the same order of magnitude as the longitudinal temperature of ions and electrons.

Positively charged ions have an additional diffusion mechanism in a transverse direction because of the generation of longitudinally bound macroscopic ion-electron pairs at their entrance into the electron beam. At a sufficiently strong magnetic field $B^2 \gg 4\pi n mc^2$, when the contribution of adiabatic collisions becomes dominant, the transverse motion of an electron in the ion-electron bound system can be taken as magnetized. In this case, the electron oscillates along the magnetic field and drifts slowly around the ion in the electric and magnetic cross fields, and the electron seems «tied down» to the magnetic field force line and to the ion. As a result, the time of ion-electron interaction increases sharply compared to the case of a negatively charged ion ($\tau^- \simeq (e^2/(mr^3))^{-1/2}$) leading to a substantially increase in the transverse diffusion. The main contribution is made by the bound pairs of the size $r \ll n^{-1/3}$, that simplifies sufficiently the calculations. Let the time of the ion existence in the electron beam be small compared to the reverse ion Larmour frequency $Mc/(eB)$. Then one can neglect the influence of the magnetic field on the ion motion and the transverse momentum transferred to the ion due to the pair generation at $v_p \ll \sqrt{2e^2 n^{1/3}/m}$ is equal to

$$\Delta \mathbf{p}_{p\perp} = \int_0^\tau \frac{e^2}{r^3(t)}\, \mathbf{r}_\perp(t)\, dt \tag{2.51}$$

where $\mathbf{r}(t)$ is the distance between the ion and the electron. Due to the drift motion of the electron the vector $\mathbf{r}(t)$ is rotating around the magnetic field direction with an angular velocity ce/r^3B. Calculating the integral we get:

$$\Delta p_{p\perp}^2 \simeq \frac{4e^2B^2r^2}{c^2}\sin^2\left(\frac{ce\tau}{2Br^3}\right). \qquad (2.52)$$

By averaging over impact parameters for the transverse diffusion coefficient we have

$$\frac{d}{dt}\langle \Delta p_{p\perp}^2 \rangle = \frac{1}{2}f_0 \int_0^{r_{max}} \Delta p_\perp^2 \frac{2\pi\rho d\rho}{\pi r_{max}^2} \simeq \frac{4e^2B^2f_0}{c^2 r_{max}^2}\int_0^\infty \rho^3 d\rho \sin^2\left(\frac{ce\tau}{2B\rho^3}\right), \qquad (2.53)$$

where $f_0 = \tau_0^{-1}$ is an ion frequency of flying in to the cooling section and the maximum size of a bound pair is determined by the mean intraparticle distance $r_{max} \simeq n^{-1/3}/2$. As a result we get

$$\frac{d}{dt}\langle \Delta p_{p\perp}^2 \rangle \simeq 6ne^4\left(\frac{\tau_0 B^2}{nc^2e^2}\right)^{1/3}, \qquad (2.54)$$

and the transverse equilibrium temperature is of the order of

$$T_\perp^+ = \frac{1}{2M\lambda^+}\frac{d}{dt}\langle \Delta p_{p\perp}^2 \rangle \simeq 5e^2n^{1/3}\left(\frac{e^2\tau^2B^4}{nm^3c^4}\right)^{1/6} = 5e^2n^{1/3}\left(\sqrt{4\pi}\frac{\tau_0\Omega_e^2}{\omega_{pe}}\right)^{1/3} \qquad (2.55)$$

where $\Omega_e = eB/(mc)$ is an electron Larmour revolution frequency. This evaluations are valid at $\omega_{pe}^{-1} < \tau_0 < \omega_{pe}^{-1}\cdot(\Omega_e/\omega_{pe})$, that is well satisfied to most of electron cooling devices. For the device NAP-M [11] $n = 2\cdot10^8$ cm^{-3}, $\tau_0 = 10^{-8}$ s, $B = 1$ kG we get $\Omega_e = 1.6\cdot10^{10}$ Hz, $\omega_{pe} = 8\cdot10^8$ Hz, $T_\perp^+ = 80e^2n^{1/3}$ that is approximately by two orders of magnitude higher than the equilibrium value for negatively charged ions.

With an increasing in the magnetic field the ion Larmour revolution radius can become smaller than the average interelectron distance that leads to a decrease in cooling decrements and hence to violation of the evaluations given. Although this corresponds to the sufficiently high magnetic fields $B > \sqrt{8Mc^2n}$, which are higher than the fields used in real devices for electron cooling.

Fig. 5 shows the dependence of the equilibrium spread of transverse velocities on the magnetic field and the transverse temperature of the electron beam taken from Ref. [25]. It is seen that the equilibrium temperature grows with an increasing in the magnetic field and electron transverse velocities. The calculations are performed with numerical simulation of single ion collisions with electrons. Although this approximation of pair collisions is too rough the

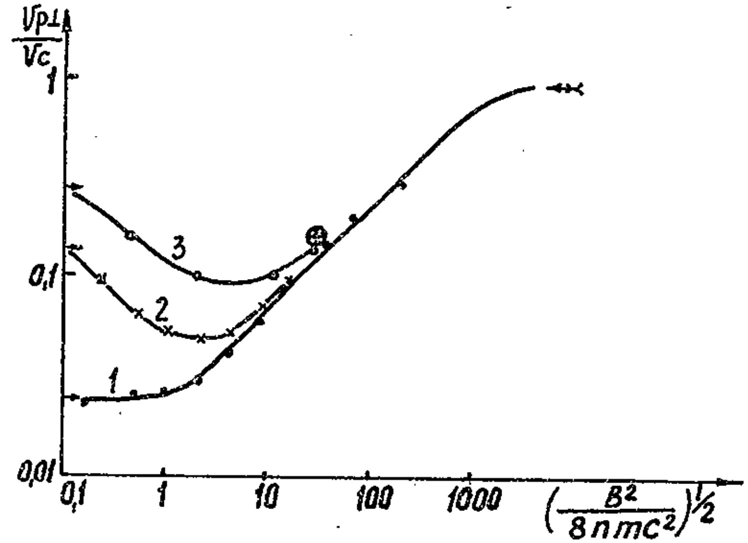

Fig. 5. Equilibrium spread for proton transverse velocities as a function of magnet field value in the cooling section for various values of electron velocity sprea $1 - \cdot - v_{e\perp}/v_c = 0$; $2 - \times - v_{e\perp}/v_c = 8$; $3 - \bigcirc - v_{e\perp} = 16$; $\oplus$ is an experimental resu obtained at cooling protons on the installation NAP-M, $v_c = \sqrt{2e^2n^{1/3}/m}$.

results of numerical calculations are in a good agreement wit those obtained experimentally on the device NAP-M.

From the estimates given above it follows that in the absence c external «warming» factors an electron cooling enables one to ob tain very small equilibrium spread for ion velocities. So if one cool antiprotons in the device with parameters similar to NAP-M (io energy 65 MeV, cooling section length 1 m, $n = 2\cdot10^8$ cm^{-3}) a equilibrium spread of velocities will be

$$\frac{v_\perp}{v_0} \simeq \frac{v_\parallel}{v} \simeq \sqrt{\frac{2e^2n^{1/3}}{Mv_0^2}} = 1.6\cdot10^{-6}.$$

For protons the longitudinal velocity spread will be the same whil the spread of transverse velocities will be approximately six time higher: $v_\perp/v_0 = 10^{-5}$.

The main effect limiting the attainment of so cooled beams i storage rings is the mutual interaction of stored ions. The interaction of particles in the transverse direction leads to the focussing attenuation and shifts the betatron frequencies to dangerous «machine» resonances that in principle limits the beam compression. The compensation for such a shift of the betatron frequencies with returning the focussing structure turns out low efficient because of a strong nonlinearity of the cooled beam field that leads to the dependence of frequency shift on the amplitude of the betatron oscillations [6]:

$$\varepsilon_{\perp} \gtrsim \frac{r_p R_0 (N/l)}{2\Delta\nu_{max}\beta^2\gamma^3}. \tag{2.56}$$

Here N/l is a number of ions per beam length unit; r_p is an ion classical radius; β, γ are relativistic factors; $\Delta\nu_{max} \simeq \simeq 0.1 \div 0.2$ is a distance to the nearest «machine» resonance; R_0 is an average radius of a storage ring.

Another effect limiting the beam cooling is an intrabeam scattering [11, 14]. This effect is connected with a mutual scattering of ions in a beam. If cooling is occured at an ion energy lower than the critical one, the intrabeam scattering leads to equalizing the ion temperature over all the degrees of freedom. In particular, while cooling positively charged ions the ion longitudinal temperature grows at the expence of the transverse temperature. In this case the diffusion coefficient for a longitudinal motion is of the order of

$$\frac{d}{dt}\langle \Delta p_{\parallel}^2 \rangle \simeq \frac{2e^4 L_C (N/l)}{v_0 \varepsilon^{3/2} \beta_f^{1/2}}. \tag{2.57}$$

Here β_f is an average value of the β-function of the storage ring, L_C is the Coulomb logarithm. Comparing the diffusion due to internal scattering with the diffusion on the electron beam (2.49) for the parameters of NAP-M device ($N=10^8$, $l=50$ m, $\beta_f=7$ m, $\varepsilon=1.3\cdot10^{-7}$ cm·rad, $n=2\cdot10^8$ cm^{-3}) we have

$$\frac{d\langle \Delta p_{p\parallel}^2 \rangle/dt}{d\langle \Delta p_{a\parallel}^2 \rangle/dt} = \frac{L_C}{2\pi}\,\frac{N v_c}{v_0 \varepsilon^{3/2} \beta_f^{1/2} l n} \simeq 10. \tag{2.58}$$

Hence it is evident that the diffusion due to the internal scattering should by nearly an order of magnitude increase the longitudinal temperature of protons. Nevertheless, in the experiments on NAP-M the strong suppression of the internal scattering was observed (see below s.3.4).

3. EXPERIMENTAL STUDY OF ELECTRON COOLING IN THE RANGE OF LOW RELATIVE VELOCITIES

In this section the results of the electron cooling experimer study performed on the device «Solenoid model» in Novosibi [10] are discussed and their comparison with the results of the f tion force measurements done on NAP-M [9] is given, and poss lities to attain the supercooled beams are considered.

3.1. «Solenoid Model» Device

A schematic view of the installation is given in Fig. 6. The of a hydrogen negative ion injector [15—17] enables one to ca out experiments both with negatively and positively charged io The change of the ion charge sign is achieved with a special pa magnesium target switched on at the solenoid entrance where

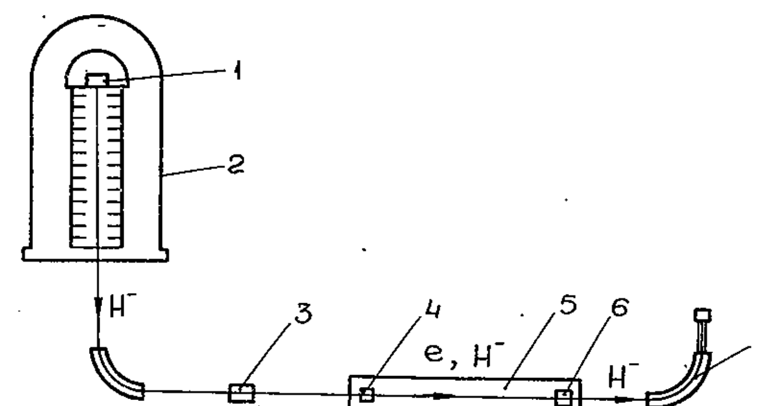

Fig. 6. Schematic diagram of installation «Model of Solenoid»; *1*—a source of H 2—electrostatic accelerator; *3*—paramagnesium target; *4*—electron gun; *5*—sc noid; *6*—collector; *7*—spectrometer; *8*—additional solenoid.

double ionization of the hydrogen negative ions occurs. In the so noid the ion beam is put in the same position in space (and dir tion and value of velocity) as an electron beam. The electron bea is formed in the electron gun [18] placed in the magnetic field the solenoid [19] and it is transported along the solenoid magne field to an electron collector. For a local change of the magne field an additional small solenoid is placed near the gun inside the main solenoid enabling to control the electron beam size in the cooling section. The interaction of ions with the electron beam results in a variation of their energy and transverse velocities. The ions after outgoing the solenoid reach the electrostatic spectrometer designed for measurements of the longitudinal friction force. The main experimental parameters are given below.

Hydrogen ion energy	850 keV.
Stability of H^- ion injector energy $\Delta\mathscr{E}_p/\mathscr{E}_p$	$\leqslant 5\cdot10^{-5}$.
H^- ion current	$\sim$1 nA.
Angular spread and radius of ion beam in cooling section	$\leqslant$0.7 Mrad$\times$0.5 mm.
Energy of electrons	470 eV.
Electron beam current	up to 15 mA.
Electron beam radius	1 mm.
Solenoid magnetic field B	1—4 kG.
Magnetic field of additional solenoid from	-2 to $+2$ kG.
Nonparallelity of magnetic field over the solenoid length	$\leqslant 5\cdot10^{-5}$.
Solenoid length	2.88 m.
Cooling section length	2.4 m.

The experiments with beams of low energy enable one to attain very small both the transverse and longitudinal relative velocities of cooling particles. So, the difference in the transverse velocities for ions and electrons due to distortions of the magnetic field $v_{\perp B}=v_0B_\perp/B$ is about $5\cdot10^4$ cm/s that is by the order of magnitude less than the characteristic spread of electron velocities $v_{e\parallel}=\sqrt{2e^2n^{1/3}/m}\approx5\cdot10^5$ cm/s. The friction force large value enables one to use a single-flight measuring scheme at relatively low energy of ions.

3.2. Measurements of Electron Longitudinal Temperature

The schematic of measurements of the longitudinal temperature [10, 12] is shown in Fig. 7. The method of measurements is based on the analysis of the energy spread in a fine electron beam cut from the main beam with a small hole ($\varnothing=0.02$ mm). The analysis is performed with a decelerating electric field of an analyzing diaphragm. By varying the analyzing diaphragm potential with respect to the cathode potential and simultaneously measuring the collector current one can obtain an integral distribution function for

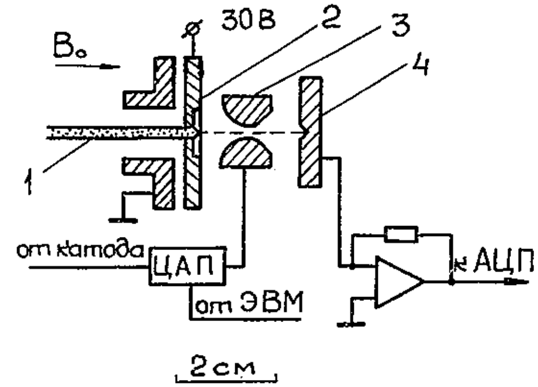

Fig. 7. Measurement scheme for electron longitudinal temperature: *1*—electr beam; *2*—cutting diaphragm; *3*—analyzing diaphragm; *4*—collector.

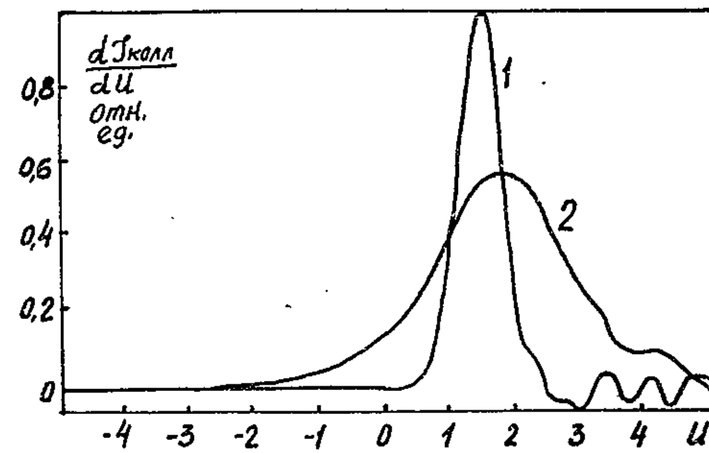

Fig. 8. dI_{coll}/dU dependence on analyzing diaphragm potential for various values electron beam current. Magnetic field $B=3$ kG, electron energy $W=470$ eV electr current: *1*—1.54 mA, *2*—5.1 mA.

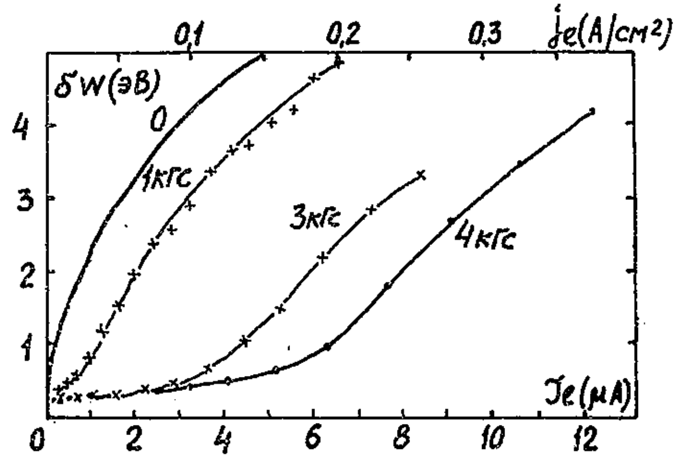

Fig. 9. Energy spread dependence for electrons at the cooling section end on electron beam current and magnetic field. Electron energy is 470 eV. *0*—is a result of calculation for magnetic field $B=0$ according to expression (2.5).

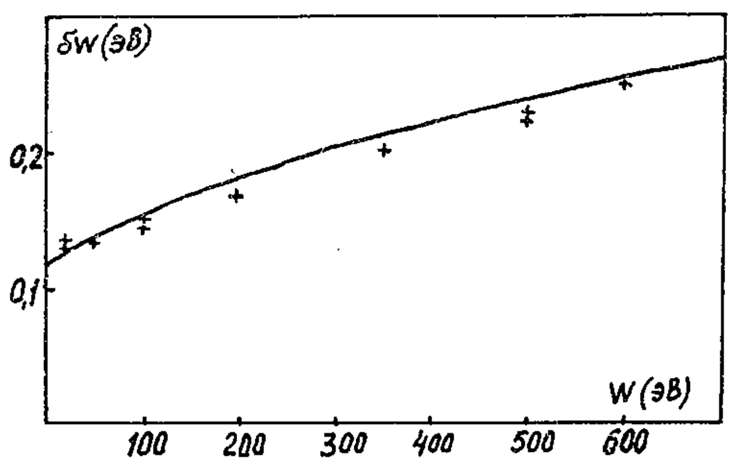

Fig. 10. Energy spread dependence for electrons δW at the end of drift section of 40 cm long of electron beam energy W for a low current of electron beam ($I_e=30$ μA). Magnetic field is 1.3 kG. Solid line is a result of culculation by formula (2.8).

electrons over their energy. Fig. 8 shows the distribution fu for electrons over the energy for two values of the electron current. It is obtained by differentiation of the integral distril function. Under the assumption of Maxwell distribution of ele over velocities with the integral distribution function the square spread of electron velocities is calculated connected wi electron longitudinal temperature $T_\parallel$ using the relation rever (2.4):

$$\delta W = (2T_\parallel W)^{1/2}.$$

At the same time the value is found out of ΔU—a shift of cen weight of the distribution function of electrons with respect cathode potential.

The main result of the experiments is a substantial depen of the beam longitudinal temperature after its passing the dri tion of the values of the electron current and magnetic field installation. Fig. 9 shows the dependence of the electron e spread at the end of the cooling section δW on the electron c I_e and the magnetic field value B in the cooling section. Exper tal curves have a characteristic form: in the region of smal rents there is a plateau whose length depends on the magneti value and at sufficiently large currents the curve comes to asy tic $I_e^{1/2}$. The presence of the plateau on the experimental curve cates the strong influence of the longitudinal magnetic field pressing the process of the transverse-longitudinal temperature xation. The plateau length increases with the growth of the These results were first obtained in Ref. [12] and are their f developments.

Experimental data on the study of the transverse-longit relaxation one can unite by an empirical formula [9]:

$$\frac{dT_\parallel}{dz} = \left(\frac{dT_\parallel}{dz}\right)_0 \exp\left[-\frac{2.8e^2}{\rho_\perp(e^2 n_e^{1/3} + T_\parallel)}\right].$$

Here $(dT_\parallel/dz)_0$ is a rate of the transverse-longitudinal rela without magnetic field according to the expression (2.5) and

$$\rho_\perp = \frac{(2T_\perp mc^2)^{1/2}}{eB}$$

is an average radius of the Larmour revolution of electror comparison with the experimental results the electron tran temperature $T_\perp$ in the expressions (3.2), (2.5) was taken to be equal to 0.11 eV and the Coulomb logarithm $L_C=6.0$. The numerical integration of the empirical formula gives a satisfactory agreement with the experimental data (within 30%, when parameters are varying in the range $B=1\div3$ kG, $I_e=0.1\div10$ mA, $W=100\div600$ eV). Because of an exponential character of the expression (3.2) for numerical integration it is essential to take correctly the temperature value $T_\parallel$ at the beginning of the cooling section which is mainly determined by the longitudinal-longitudinal relaxation. One should make with a certain care the extrapolation of (3.2) for a wider range of parameter values.

At a low beam current and a strong magnetic field the process of the transverse-longitudinal relaxation is strongly suppressed and the longitudinal temperature in the electron beam is determined by the longitudinal-longitudinal relaxation. Fig. 10 shows the dependence of a spectrum width on the energy of electrons. If there is no mutual interaction between electrons the spectrum width should not depend on the electron energy and should be of the order of the cathode temperature value (1200K$\simeq$0.11 eV). Nevetheless, the experimental data given in Fig. 10 show that the spectrum width is noticeable higher than the cathode temperature and grows with the increase in the electron energy. This dependence is opposite to that observed in the case of the transverse-longitudinal relaxation when with the energy growth the spectrum width becomes smaller. The obtained experimental data on the longitudinal-longitudinal relaxation are well described by expressions (3.1) and (2.8) at $C=2$: $\delta W=\sqrt{2T_\parallel W}\simeq\sqrt{T_c^2+4We^2n^{1/3}}$.

Note that with the beam acceleration in the electron gun the main contribution into an increase in the longitudinal temperature is made by the longitudinal-londitudinal relaxation. As a rule, the contribution of the transverse longitudinal relaxation is insignificant even in the absence of a magnetic field and the longitudinal temperature the electron gun output is determined by (2.8). In this case of the Piers gun one can easily evaluate the relative contribution of both the summands. By adding an adiabatic cooling due to acceleration $dT_\parallel=-T_\parallel\frac{dW}{W}$ (see (2.4)) into expression (2.5) we get the differential equation describing the variation of longitudinal temperature during the acceleration in the gun taking into account the transverse-longitudinal relaxation:

$$\frac{dT_\parallel}{dz}=-\frac{T_\parallel}{W}\frac{dW}{dz}+\frac{\pi e^3 jL_Ck}{W}\sqrt{\frac{m}{T_\perp}},\quad \frac{d}{dz}(T_\parallel W)=\pi e^3 jL_Ck\sqrt{\frac{m}{T_\perp}}. \quad (3.4)$$

By integrating (3.4) from the cathode surface $z=0$ to the anode $z=a$, we get the gun output temperature that comprises the contribution of the transverse-longitudinal relaxation:

$$T_\parallel^{(1)}=\frac{T_c^2}{2W}+\frac{\pi e^3 jkL_Ca}{W}\sqrt{\frac{m}{T_\perp}},\qquad T_\perp\simeq T_c. \quad (3.5)$$

The contribution of the longitudinal-londitudinal relaxation $T_\parallel^{(2)}$ is determined by expression (2.8). The relation is equal to

$$\frac{T_\parallel^{(1)}}{T_\parallel^{(2)}}\simeq\frac{\pi L_Ck}{\sqrt{18\pi}}\sqrt{\frac{e^2n^{1/3}}{T_\perp}}\simeq 2.7\sqrt{\frac{e^2n^{1/3}}{T_c}},\quad T_\parallel^{(1)},\ T_\parallel^{(2)}\gg\frac{T_c^2}{2W}. \quad (3.6)$$

Here an energy W is taken to be sufficiently high so the cathode temperature contribution can be neglected and for the Pierce gun the relation between current density and voltage is taken into account (law «3/2»):

$$j=\frac{1}{9\pi}\sqrt{\frac{2}{m}}\frac{W^{3/2}}{ea^2}. \quad (3.7)$$

At a density of electrons $n\simeq10^9$ cm^{-3} the transverse-longitudinal relaxation contribution is of the order of 0.1 from the contribution of the longitudinal-londitudinal relaxation. This estimate does not take into account the suppression of the transversal-longitudinal relaxation by a strong magnetic field, therefore in the real experiment its contribution will be even substantially smaller.

The variation of the beam current and the electron gun heat current leads to the shift of the centre of weight for the distribution function ΔU which is caused by the following effects. First, it is the dependence of the potential minimum near the cathode on relaxation to the beam current and the cathode saturation current. According to (2.3) the variation of the gun current or the cathode emitting capability (with heat current tuning) leads to the shift of the spectrum centre of weight. Second, it is a decrease in potential of the emitting surface with a growth of the electron current connected with a resistence of the cathode oxide layer which under our conditions is of 20—70 Ω and depends strongly on the cathode temperature [26]. In this case, the resistence of the conductor carrying the current to the cathode of the order 1 Ohm can be neglected. Third, it is the contact difference of potentials U depending on the temperatures.

Fig. 11 shows the dependence of the position of the spectrum centre of weight on the gun current during the gun operation in the

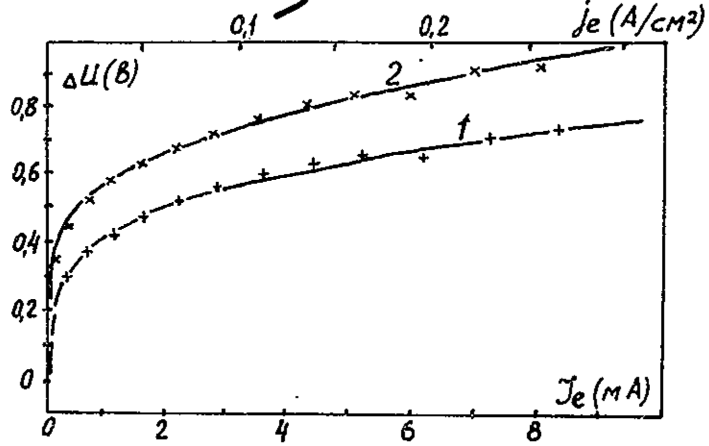

Fig. 11. Distribution function centre of weight shift ΔU dependence on electron beam current for various values of electron gun heat current: *1*—350 mA, *2*—300 mA. Curves are obtained by the method of least squares with expression (3.8).

	Heat current	$U_0(V)$	R(Om)	T_c(eV)
1	0.35	0.416	13.3	0.104
2	0.3 A	0.564	23.2	0.096

«mode 3/2». The continuous curve corresponds to a fitting by the method of least squares to the expression

$$\Delta U = U_0 + RI_e + \frac{T_c}{e}\ln I_e. \qquad (3.8)$$

The value of the fitting parametres U_0, R, T_C are given in the figure caption.

The given method for measuring the longitudinal temperature is rather simple, provides a high accuracy of measurements and enables one to determine various characteristics of the electron beam and the electron gun. In Ref. [18] this method has been used for studying optical properties of the electron gun. The idea of the

experiment is based on the fact that excitation of transverse velocities of electrons in the gun with a constant total energy leads to the shift of the centre of weight of the distribution function whose value depends on the radial position of the emitting point. At present, this method is apparently most accurate for measuring optical properties of an electron gun in a strong magnetic field.

3.3. Longitudinal Friction Force Measurement

The longitudinal friction force value is determined with the use of an electrostatic spectrometer by measuring the ion energy after its passage through the cooling section. To this purpose at a given ion injector energy the energy dependence of ions outgoing the solenoid on the electron energy is measured. With the same values for the ion and the electron beam velocities the friction force value is equal to zero, and the ion energy does not change, when the electron energy deviates from its equilibrium value the friction force occurs leading to the change of the ion energy. The energy change value δE_i proportional to the friction force value $F_\parallel$ and to the length of the cooling section ($\delta E_i = F_\parallel \cdot l_c$). The relative value for the ion energy variation is small ($\delta E_i/E_i \leqslant 5\cdot 10^{-5}$) and it is comparable with the stability of the accelerating voltage of the ion injector. To seperate a useful signal on the background of the accelerating voltage noise the multiple measurements were performed whose results are summarized. The duration of a single measurement was 0.2 s and a total number of measurement in a cycle is 1000. Fig. 12 shows an example of the obtained in such a way dependence of the energy variation for H^- and H^+ ions on the electron beam energy at a magnetic field of 4 kG and current of 3 mA. As it is seen the friction force value for negative ions is about 2.5 times larger than that for positive ions.

The dependence of the ion energy variation on the electron energy both for positively and negatively charged particle is in a good agreement with the following semiempirical formula (see (2.16)):

$$\delta\varepsilon_i(\delta\varepsilon_e) = \delta\varepsilon_{i\,\max}\frac{25\sqrt{5}\,\Delta E_0^4\,\delta\varepsilon_e}{16(\Delta E_0^2+\delta\varepsilon_e^2)^{5/2}}, \quad \delta\varepsilon_{i\,\max} = F_{\max} l_c \qquad (3.9)$$

that is used for finding out the maximum value for the friction force $F_{\max}(\delta\varepsilon_{i\max})$ and the characteristic energy width ΔE_0 with the method of least squares by the measured dependence.

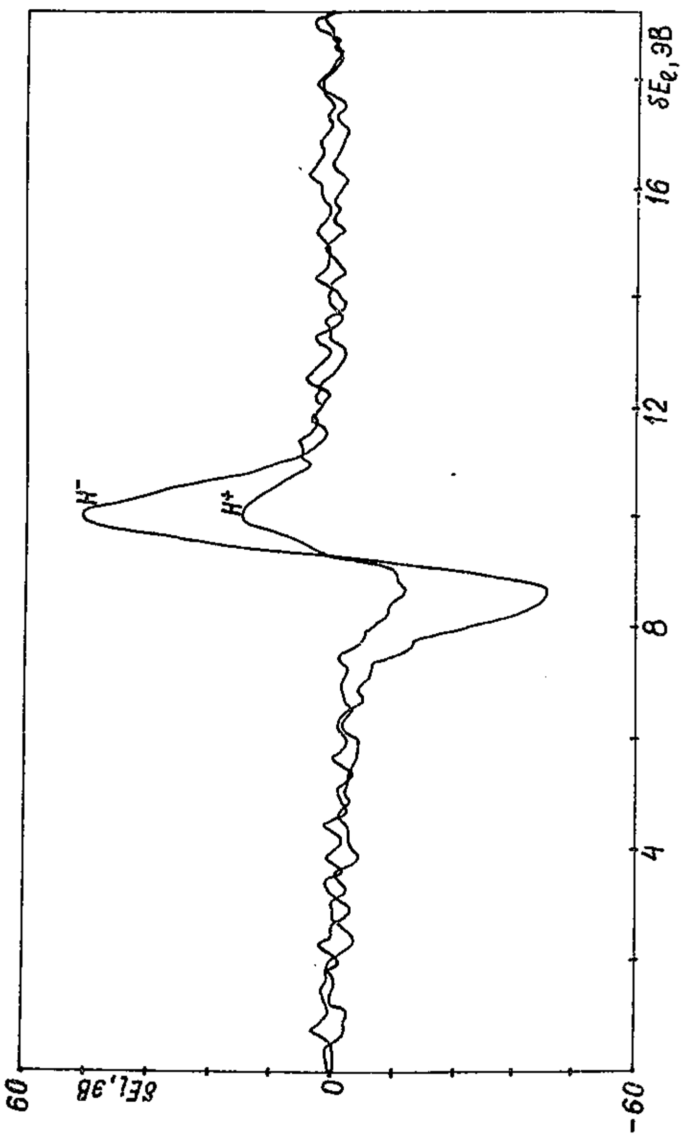

Fig. 12. Dependence of energy variation for ions of various charge signs on electron energy, $B=4$ kG, $I_e=3$ mA.

Fig. 13 shows the maximum longitudinal friction force as a function of the electron beam current for ions of various signs (p, H^-) and of the magnetic field being equal to 3 kG. With an increase in current the friction force grows up and attains its maximum value at a current of the order of 4—5 mA. With a further current increase the friction force starts to decrease. A decrease in the friction force with the growth of the electron current can be explained by the action of various factors whose relative contribution is hard to define. First, it is a growth of the electron longitudinal temperature along the beam length determined by internal collisions in an electron flux. Second; it is the absence of a complete compensation of the space charge of the electron beam that leads to the defocussing (focussing for H^+) of the ion beam by a radial electric field and to the enhancement of their transverse velocities on the cooling section and also an excitation of the ion transverse velocities on the input section as a result of the effect of a noncompensated electron beam on the ion beam in the electron gun. Third, it is an influence on the friction force of the electron velocity gradient along the radius connected with an action of the beam space charge. In the region of low currents these factors are insignificant and the dependence of the maximum friction force F_{max} on the density is in a good agreement with the following expression

$$F_{max} = C_F e^2 n^{2/3} \tag{3.10}$$

(see (2.44), (2.45)).

The friction force measurements have been carried out for magnetic fields ranging from 1 to 4 kG. Fig. 14 shows the relation $F_{max}/e^2n^{1/3} = C_F$ as a function of a magnetic field value in the cooling section. This relation is calculated in the range of low currents of the electron beam where the dependence of the maximum friction force on the current is in a good agreement with expression (3.10). This figure shows also the electron beam current I_{ext} at which the friction force attains its maximum value (with a variation of the electron beam current and a constant value of the magnetic field).

According to Fig. 14 at a field value of 1 kG the friction force values are the same both for positively and negatively charged particles and with an increase in the magnetic field value the friction force for H^- grows up strongly while for H^+ it remains nearly the same. The weak dependence on the magnetic field of the friction force for positively charged ions already indicated the strong mag-

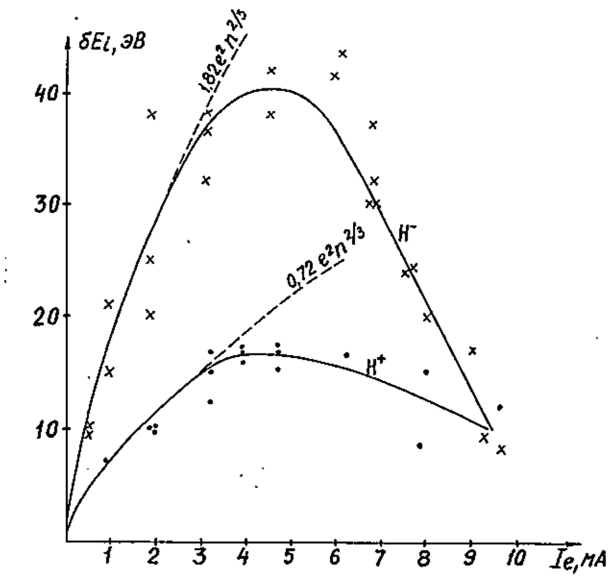

Fig. 13. Dependence of ion energy maximum variation on electron current, $B=3$ kG, $\times$—H$^-$, $\cdot$—H$^+$, cooling section length $l_c=2.4$ m. Dashed lines are obtained with the use of the following expressions: $F^-_{max}=1.82e^2n^{2/3}$, $F^+_{max}=0.72e^2n^{2/3}$.

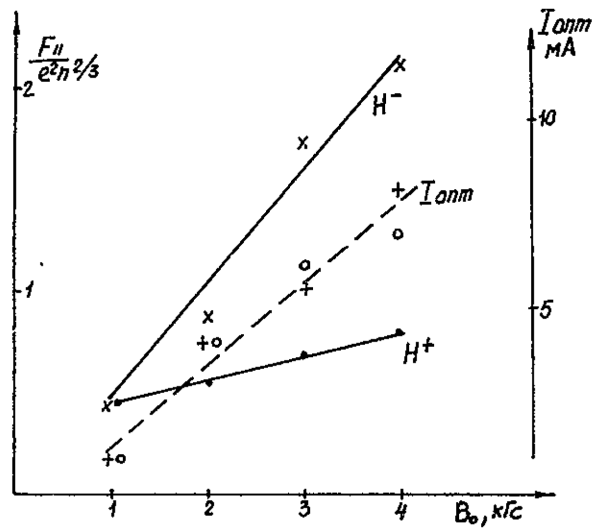

Fig. 14. Dependence of relation $F_{max}/e^2n^{2/3}$ for low currents of electron beam ($\times$—H$^-$, $\cdot$—H$^+$) and of electron beam current I_{ext} at which longitudinal friction force F_{max} attains its maximum (+, ○) on magnetic field.

netization of collisions and it seems to be connected with a slight improvement in the electron and the ion beam quality. At the same time for negatively charged particles the friction force increases substantially with the growth of the field and the difference in the friction force values for H$^+$ and H$^-$ is large for strong magnetic fields.

Another important characteristic of the friction force is the characteristic width ΔE_0 of its energy dependence. At a small angular divergence of the ion beam and a sufficiently low longitudinal temperature of electrons ($T_\parallel \lesssim 2e^2n^{1/3}$) this width is determined by the density of electrons (see (2.43)). An increase in the longitudinal value due to the transverse-longitudinal relaxation leads to an increase in ΔE_0. Fig. 15 shows ΔE_0 as a function of the electron beam energy for various values of the magnetic field. In the area of high intensity of the field and low currents of the electron beam, when the transverse-longitudinal relaxation can be neglected, the dependence $\Delta E_0(I_e)$ is in a good agreement with the expression

$$\Delta E_0 = \sqrt{32We^2n^{1/3}}. \qquad (3.11)$$

Hence, the friction force achieves its maximum F_{max} when the ion longitudinal velocity deviates at a value equal to:

$$v_F = 2\sqrt{\frac{e^2n^{1/3}}{m}} = \sqrt{2}\, v_c \qquad (3.12)$$

(compare with 2.43)) that exceeds noticeably the heat spread of electron velocities.

With an increase in the electron current the characteristic energy width grows the larger the lower is a magnetic field. This is determined by amplifying the transfer of the electron transverse motion into its longitudinal motion, i. e. by an increase in the longitudinal temperature which determines the characteristic energy width.

By comparing Figs. 9 and 15 it is evident that changes in ΔE_0 behaviour from formula (3.11) occur at an electron beam current determined by an equality of the characteristic energy width ΔE_0 to an energy spread for electrons at the end of the cooling section. So, at $B=3$ kG an energy spread for electrons starts to grow at $I_e \simeq 3$ mA and the changes in behaviour of ΔE_0 and of the maximum friction force F_{max} occur at $I_e \simeq 5$ mA when an energy spread for electrons becomes comparable with the characteristic energy width.

More distinctly it is seen from Fig. 16 where the results of

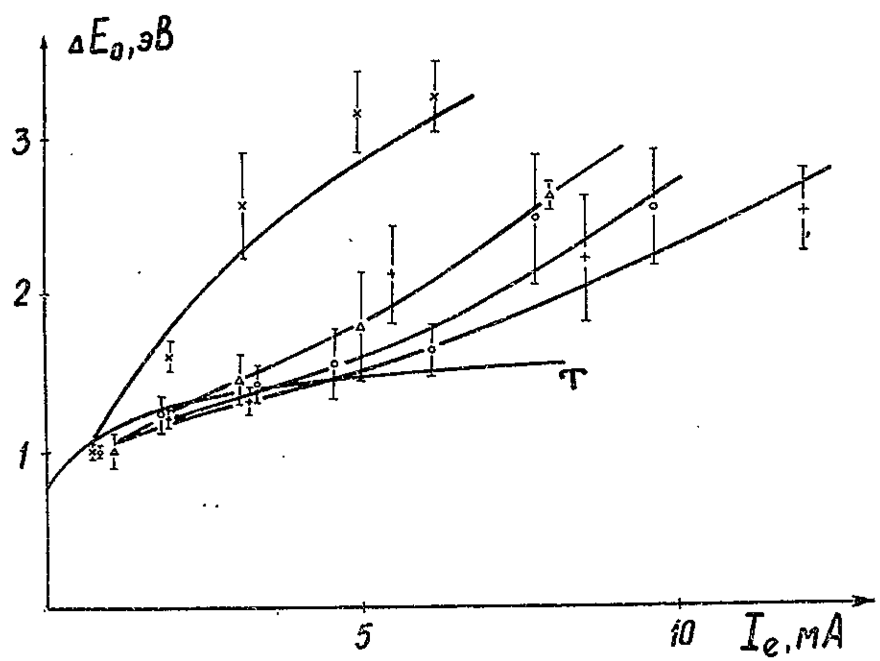

Fig. 15. Dependence of energy width ΔE_0 of the friction force on electron current for different magnetic fields: 4 (+), 3 (○), 2 (△) and 1 kG (×); values ΔE_0 for positively and negatively charged ions coincide with an accuracy of measurement. The dashed line T is obtained with the help of expression $\Delta E_0 = \sqrt{32 W e^2 n^{1/3}}$.

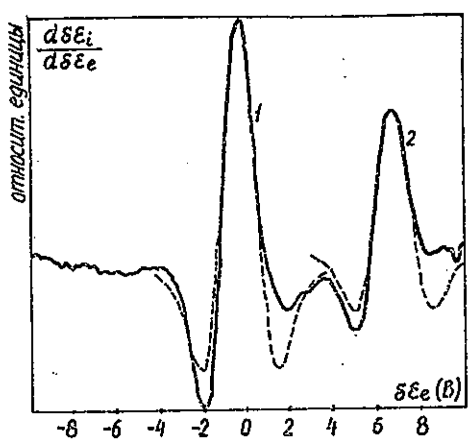

Fig. 16. Relative contribution into the total value of friction force from parts of electron beam at the beginning (length 140 cm) and at the end (length 70 cm) of the cooling section. Full length of cooling section is 140 cm+70 cm=210 cm.

measurements of the friction force generated by two different cooling sections: an «input» section ($0 \leqslant Z \leqslant 140$ cm) and an «output» one (140 cm$\leqslant Z \leqslant$210 cm) are given. In order to separate the contribution into the friction force from each of the areas the ions compensating the electron beam were removed out from one of the areas. As a result the area potential and consequently, an electron average velocity are decreased, so friction force from this noncompensated area is observed at higher voltages on the electron gun cathode. In order to avoid systematic errors the ion compensation was taken off first from one and then from the other part of the electron beam. The measurements were carried out with using a synchronous detection of the signal proportional to the variation of the ion energy. The signal was excited by applying alternating voltage to the cathode of the electron gun (270 Hz, 0.5 V—amplitude). The result of these measurements is a derivation of the longitudinal friction force over the electron beam energy given in Fig. 16. The dashed line is a fitting by the method of least squares to the derivation of (3.9). An independent processing of peaks gives the following values:

	Z (cm)	$\Delta\varepsilon_i$ (eV)	ΔE_0 (eV)	F_{max} (eV/m)
1	0—140	22.9	1.25	16.3±2
2	140—210	13.2	1.26	18.8±2

The electron beam current is 3.2 mA, the magnetic field is 3 kG, the particles cooled are ions H^-.

As an example let us give a comparison of the results obtained on the friction force measurements with the results obtained on the NAP-M installation. The maximum value for the longitudinal friction force obtained on NAP-M was of the order of 0.5 eV/m at a density of electrons $n_e = 2 \cdot 10^8$ cm^{-3}. This force was obtained with the difference in longitudinal velocities of beams of the order of $8 \cdot 10^5$ cm/s. Using the given in Fig. 14 and expressions (3.9) and (3.12) we obtain $F_{max} \simeq 0.45 e^2 n^{2/3} = 2.36$ eV/m, $v_F = 2\sqrt{e^2 n^{1/3}/m} = 3.9 \cdot 10^5$ cm/s, and the friction force with the velocity difference $v_p = 8 \cdot 10^5$ cm/s is equal to

$$F_{\parallel}(v_p) = \frac{25\sqrt{5}}{16} F_{max} \frac{(2v_F)^4 v_p}{((2v_F)^2 + v_p^2)^{5/2}} = 1.4 \text{ eV/m}.$$

A three times lower value of the friction force obtained on the NAP-M installation was caused by the nonparallelity of the magnetic field force lines along the cooling section: $\Delta B_{\perp}/B \simeq 2 \cdot 10^{-4}$. This leads to an additional difference in the beam transverse velocities: $\Delta v_{\perp} \simeq 2 \cdot 10^6$ cm/s and consequently to a decrease in the friction force in the range of low velocities. For the installation «Solenoid model» the relative transverse velocities for ions are lower than 10^6 cm/s. The measurements carried out of transverse velocities have shown that the friction force starts to decrease at $v_{\perp} > 10^6$ cm/s.

3.4. Equilibrium Values for Velocity Spread in Beams

The experimental measurements of the equilibrium values for the velocity spread have been performed on the NAP-M installation [20]. The transverse spread $(\Delta p_{\perp}/p)$ was found out with measurements of the transverse size of the cooled beam. For this purpose, the proton beam was crossed with a fine quartz filament and an emission current $I(t)$ of secondary electrons from the filament was detected. At a beam energy of 65 MeV the cooled beam diameter was 0.22 mm and increased weakly with growth of the proton beam current up to 40 μA. The whole diameter value corresponds to the beam angular spread $\theta_{\perp} = \frac{\Delta p_{\perp}}{p} \approx 1{,}2 \cdot 10^{-5}$ (β-function for NAP-M

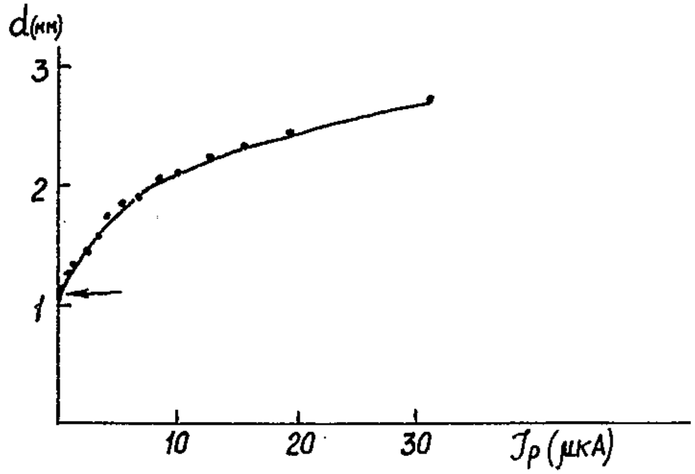

Fig. 17. Dependence of proton beam diameter on its current at an energy of 1.5 MeV. Electron beam current is 1 mA. Experiments on NAP-M. An arrow shows the calculated value of diameter at $I_p \to 0$ with expression (2.55), $(T_{\perp}^{+} \simeq 330 e^2 n^{1/3} \simeq 10^{-2}$ eV).

is equal to 7 m) and the transverse velocity in an accompanying coordinate system is $v_{\perp} \approx 1.3 \cdot 10^{+5}$ cm/s. At an energy of the beam 1.5 MeV the strong growth of diameter was observed from 1 mm at a low proton current up to 2.7 mm at a current of 30 μA as shown in Fig. 17. The equilibrium value of the transverse velocity at $I \to 0$ was $\theta_{\perp} = 7 \cdot 10^{-5}$, $v_{\perp} \approx 1.2 \cdot 10^5$ cm/s. The effect of increasing the transverse size with the growth of the proton current is apparently connected with an influence of machine resonances as the shift of betatron frequency due to the field of a specific space charge becomes comparable with a distance to the nearest integer resonance.

The equilibrium values of the electron beam transverse velocities at a low current correspond quite well to the values of (2.55). The beam longitudinal velocity spread was measured by the level of heat noise induced on pick-up electrodes. The voltage induced in the circular pick-up electrode is proportional to the local density of a beam

$$\rho(\theta, t) \approx \sum_{a=1}^{N} \delta(\theta - \theta_a(t)) = \sum_{n=-\infty}^{\infty} A_n \exp(in\theta)/2\pi ,$$

$$A_n = \sum_{a=1}^{N} \exp(-in\theta_a(t)) . \qquad (3.13)$$

where $\theta_a(t)$ is an azimuthal position of an a-particle of a beam consisting of N particles. Taking into account the interaction of particles the amplitude dispersion of harmonics A_n or the beam noise level at a friquency nf_0 one can write in the form [21]

$$\langle |A_n|^2 \rangle = \frac{N \cdot N_{th}}{N + N_{th}} = \begin{cases} N, & N \ll N_{th} , \\ N_{th} = \dfrac{\pi R_0 (\Delta\omega)^2}{e^2 \omega_0 d\omega / dp Z_n} & N \gg N_{th} , \end{cases} \qquad (3.14)$$

where R_0 is a mean radius of the storage ring. Z_n is an an impedance of chamber on the n-th harmonics of the revolution frequency (for the flat chamber $Z_n = \ln(a/r_b)/v_0\gamma$), $\Delta\omega$ is a revolution frequency spread. At a small number of particles $N \ll N_{th}$ the noise signal power $\langle |A_n|^2 \rangle$ is proportional to the number of particles — the so called Schottky noise of a beam. For the opposite ultimate case $N \gg N_{th}$ the noise power does not depend on the number of particles and it is proportional to the beam temperature. Such a decrease in the noise power is connected with the fact that the potential energy for the fluctuation density becomes much larger than the kinetic energy of a particle motion and the ordering of particles along the orbit begins to appear. At a storage ring energy higher than the critical one $d\omega/dp<0$ the self-bunching of the cooled beam particles occurs: $N_{th}<0$ (the effect of a negative mass). But even at $N_{th}>0$ in order to obtain the beam stability one should take special measures to eliminate interactions with parasitic resonators.

What is happening with a spread $\Delta p_{\parallel}/p$ under the condition when $N_{th}>0$ and the stability conditions are satisfied? Fig. 18

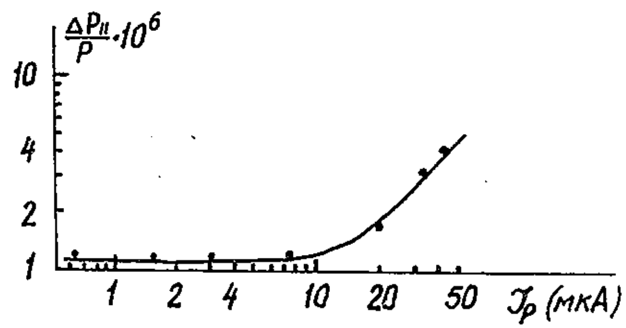

Fig. 18. Dependence of longitudinal momentum spread of proton beam on its current in NAP-M storage ring. Proton energy is 65 MeV, electron current is 0.3 A.

shows the results of measurements $\Delta p_{\parallel}/p$ on the NAP-M installation for various numbers of protons in a beam ($pc=355$ MeV, $I_e=0.3$ A, $\lambda_{\perp}=10\ s^{-1}$, $\lambda_{\parallel}=130\ s^{-1}$). It is seen that up to the proton current value of 10 μA the spread value is the same and it is equal to $\Delta p_{\parallel}/p\approx 10^{-6}$ and with a further increase in the number of particles it starts to grow. The value $\Delta p_{\parallel}/p\approx 10^{-6}$ is in a good agreement with the effective temperature in an accompanying system $T_{eff}=2e^2n_e^{1/2}\approx 1$K. Although at the beam current values described the intrabeam proton scattering should be noticeably stronger displayed leading to the heat $\Delta p_{\parallel}/p$. A weak influence of intrabeam scattering at the beam current value $I<10$ μA may be connected with the suppression of this scattering due to ordering particles in a beam. Specifically, the condition $N\gg N_{th}$ means that the fluctuation potential energy is much higher than the kinetic energy of the

chaotic motion that leads to the occurence of ordering in a beam. The suppression of the intrabeam scattering is an evidence of that the ordering is displayed up to microlevel causing a noticeable correlation in positions of neighbouring particles. In fact, the maximum potential energy of mutual repulsion for the protons oscillating with a betatron amplitude a is by the order of magnitude equal to $2e^2/a$ that under the condition of this experiment is $2.9\cdot 10^{-5}$ eV. The kinetic energy of the longitudinal motion is an accompanying system $\Delta p_{\parallel}^2/2M_s$ (where M_s is a synchrotron mass being equal to $0{,}08M_p$ for NAP-M) installation is $0.6\cdot 10^{-5}$ eV. As is seen, the potential energy of mutual repulsion is noticeably higher than the kinetic energy of a heat motion that will evidently lead to ordering at a small number of particles $N<2\pi R_0/a=0.5\cdot 10^6$. At a larger number of particles N when the longitudinal distance between particles $\Delta_{\parallel}=2\pi R/N$ becomes substantially lower than the amplitude of transverse oscillations a, the process of proton interactions becomes more complicated [22, 25]. In the experiments the suppression of the internal scattering down to the proton current level 10 μA ($N=2.8\cdot 10^7$) was observed which corresponds to the case when the longitudinal distance $\Delta_{\parallel}=1.7\cdot 10^{-4}$ cm at $a=10^{-2}$ cm.

4. ULTIMATE POSSIBILITIES OF ELECTRON COOLING

For the standard thermodiffusion cathode the temperature of electrons emitted from its surface is determined by its temperature and is of 0.1 eV. Some information appeared recently on the development of photocathodes enabling to get electrons with ultimately low temperatures [23]. The ultracooled electron beams are emitted from the surface of a crystal ArGa subjected to infrared radiation (1 μm) and cooled down to the temperature of liquid nitrogen. To decrease the gain function an atomic layer of $Cs+O_2$ is laid on the crystal surface. Such photocathodes have a high quantum efficiency (~1%). The ultimately low energy spread of emitted electrons obtained experimentally [23] is 0.03 eV (300K). In this section the possibility of keeping such low temperatures while the formation and transportation of the electron beam as well as some additional possibilities when using such electron beams for electron cooling will be discussed.

4.1. Electron Beams with the Superlow Temperature of Electrons.

Let us assume that the magnetic field is rather high and one can neglect both an increase in the transverse temperature during the beam acceleration in a gun (due to nonideal optics) and the transverse-longitudinal relaxation in the drift section. In this case, an increase in the longitudinal temperature will occur because of the longitudinal-longitudinal relaxation.

For obtaining the estimates for the longitudinal temperature one should find out the dependence of potential (correlational) energy of the electron gas on its temperature. In the high temperature region $T \gg e^2 n^{1/3}$ the expression for correlational energy is well known [24]:

$$E_{cor} = -\frac{e^2}{2}\sqrt{\frac{4\pi n e^2}{T}}, \qquad T \gg e^2 n^{1/3}. \tag{4.1}$$

For the sake of simplicity here and below we take that the space charge of the electron beam is compensated for the ion positive charge: the ions are travelling fast along the electron and therefore the ion charge density can be taken homogeneous in the region occupied by the electron beam. At low temperature the electron beam is crystallized and the correlational energy is equal to:

$$E_{cor} \simeq -Ce^2 n^{1/3} + \frac{T_\parallel}{2}, \qquad T \ll e^2 n^{1/3}. \tag{4.2}$$

The coefficient 1/2 in the second attend is connected with the magnetization of transverse degrees of freedom and a constant C is determined by the grid type. The state with the minimum energy is achieved for a volume-centred grid for which $C \simeq 1.4$. For other types of grids the value of C will be somewhat less. For the most densest gexagonal grid $C \simeq 1.38$. For the evaluation let us choose the dependence of correlational energy on the temperature in the following form:

$$E_{cor} = -e^2(\pi n)^{1/3}\sqrt{\frac{e^2(\pi n)^{1/3}}{e^2(\pi n)^{1/3} + T_\parallel}}. \tag{4.3}$$

The asymptotics of expression (4.3) are the same as those for (4.1) and (4.2). The total internal energy of the thermodynamically equilibrium magnetized electron gas is

$$E \simeq \frac{T_\parallel}{2} - e^2(\pi n)^{1/3}\sqrt{\frac{e^2(\pi n)^{1/3}}{T_\parallel + e^2(\pi n)^{1/3}}}. \tag{4.4}$$

If the acceleration is made fast compared to the period of plasma oscillations, the relative positions of electrons do not change during the time of accelaration and the initial state is kept with chaotic disposition of electrons for which the correlational energy is close to zero. This fact is due to the electron longitudinal temperature near the cathode surface is much higher than $e^2 n^{1/3}$ and there is no correlation in positions of electrons (even for the photocathode mentioned above). By equalling the internal energy of electrons just after establishing the thermodynamic equilibrium we get an equation determing the electron longitudinal temperature:

$$\frac{T_c^2}{2W} = \frac{T_\parallel}{2} - e^2(\pi n)^{1/3}\sqrt{\frac{e^2(\pi n)^{1/3}}{T_\parallel + e^2(\pi n)^{1/3}}}. \tag{4.5}$$

For the most typical case of the electron acceleration up to a high energy W ($T_c^2/2W \ll e^2 n^{1/3}$) in the left-hand part one can take $T_c = 0$; then the equilibrium longitudinal temperature is:

$$T_\parallel \simeq 1.9 e^2 n^{1/3}. \tag{4.6}$$

In the case of sufficiently slow acceleration (see below (4.10) the plasma oscillations have enough time to mix the density fluctuations and the longitudinal temperature can be much lower. The change of the electron internal energy acceleration by a value dW is:

$$dE = -T_\parallel \frac{dW}{2W} + \frac{1}{3} U \frac{dn}{n} = T_\parallel \frac{dn}{n} + \frac{1}{3} U \frac{dn}{n}, \tag{4.7}$$

where U is the potential energy whose reference value is the energy value at zeroth temperature:

$$U(T_\parallel) = E_{cor}(T_\parallel) - E_{cor}(0). \tag{4.8}$$

Hence, we have a differential equation describing the temperature variation during acceleration:

$$\left(\frac{1}{2} + \frac{\partial U}{\partial T}\right) dT_\parallel = \left(T_\parallel + \frac{1}{3} U\right) \frac{dn}{n}. \tag{4.9}$$

Fig. 19 shows the solution of this equation in dimensionless variables. During the integration the correlation energy was chosen in the form (4.4) At $T_{\parallel} \gg e^2 n^{1/3}$ the longitudinal temperature falls down rather rapidly with the growth of electron energy: $T_{\parallel} \propto 1/W$.

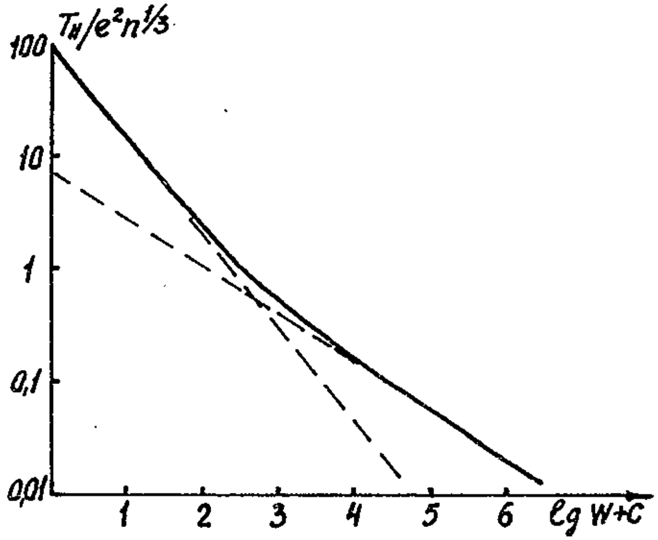

Fig. 19. Variation of the electron beam longitudinal temperature at an adiabatic acceleration as a function of the electron energy variation. C is the constant of integration. The dashed lines show asymptotics in the regions of low and high temperatures.

Although, with a decrease in temperature the derivation $|dT_{\parallel}/dW|$ also decreases and at $T_{\parallel} \ll e^2 n^{1/3}$ the temperature variation is proportional to $T_{\parallel} \propto 1/W^{7/12}$.

The acceleration adiabaticity criterion with respect to plasma oscillations has the following form:

$$\lambda = \frac{1}{\omega_{pe} T_{\parallel}} \frac{dT_{\parallel}}{dt} \ll 1, \tag{4.10}$$

where ω_{pe} is a plasma frequency of electron. During the acceleration of electrons in a gun operating in the «mode 3/2» (and more than that for the gun operating in the mode of emission limitation) the adiabaticity condition is not satisfied. In fact, neglecting the interaction of electrons we have:

$$\lambda = \left| \frac{1}{\omega_{pe}} \frac{dT_{\parallel}}{T_{\parallel} dt} \right| = \left| \frac{v}{\omega_{pe} W} \frac{dW}{dz} \right|. \tag{4.11}$$

Substituting here the dependence of the electron plasma frequency their velocity v and energy on the longitudinal coordinate z for the case of Pierce gun we get: $\lambda_{\text{Pierce}} = 2\sqrt{2}$. Thus, such an acceleration is a fast one with respect to plasma oscillations and consequently, the minimal longitudinal temperature during the acceleration in the case of Pierce gun is limited by the order of $2e^2 n^{1/3}$ (see. (4.6)).

The electron longitudinal temperature does not vary during acceleration if the gun has a sufficiently good electron optics. So, an electron gun suggested in Ref. 18 with a smooth optics enables one to limit the perturbation of transverse velocities during acceleration in the gun by the value not higher than the drift velocity of electrons in the beam electric field:

$$v_{\perp} \lesssim v_{\text{dr}} = \frac{2cI_e}{Bv_0 a_e}, \tag{4.12}$$

where v_0 is an electron velocity; a_e, I_e are the radius and current of an electron beam respectively; B is a magnetic field in the cooling section; c is the velocity of light. The requirement to the transverse drift velocity of electrons on the beam boundary to be not in excess of $v_e \equiv 2\sqrt{e^2 n^{1/3}/m}$ determines the maximum of electron density in the cooling section:

$$n \lesssim \left(\frac{B^2}{4\pi^2 mc^2 a_e^2} \right)^{3/5}. \tag{4.13}$$

The compensation for the space charge of an electron beam enables decreasing an electron drift velocity but the perturbation of longitudinal velocities in a gun cannot be done much less than v_{dr} [18].

Another effect limiting an electron beam monochromaticity is the gradient along the radius of the electron longitudinal velocity induced by the beam electric field:

$$\frac{dv_{\parallel}}{dr} = \frac{eI_e}{mv^2 a} \frac{r}{a} = \frac{2eI_e}{W} \frac{r}{a^2}. \tag{4.14}$$

In particular, this relation determines the electron energy minimum value $W_{\min}$ for starting adiabatic acceleration. From the adiabaticity condition it follows that the acceleration rate should be much less than that for the Pierce gun. In this case, an electron space charge produces the transverse electric field which cannot be compensated by the varying the shape of external electrodes. Nevetheless, by the use of the magnetic field to prevent the beam transverse repulsion one can succed in accelerating the beam sufficiently slow (according to the condition (4.10)). In this case, the beam current is limited by the condition of formation of virtual cathode in the plane where an adiabatic acceleration starts ($W = W_{min}$):

$$I_e < 2\sqrt{\frac{2e}{m}}\left(\frac{W_{min}}{e}\right)^{3/2}. \tag{4.15}$$

The magnetic field intensity in a gun should be rather high in order to suppress an increase in the electron transverse velocity during the acceleration (see (4.12)). With an increase in the electron energy the influence of a space charge decreases together with the decrease in the transverse velocity of particles.

Let us give a numerical example. Let the energy of electrons be $W=470$ eV, magnetic field $B=3$ kG, electron beam radius $a_e=1$ mm. Then from (4.13) we get the maximum density in the cooling region $n_e=5\cdot10^8$ cm^{-3}, electron beam current $I_e=3.5$ mA and the energy for starting an adiabatic acceleration $W_{min}\simeq 14$ eV. Let us assume an energy spread near the cathode to be $\Delta E_\parallel \simeq T_c = 0.03$ eV then after fast acceleration up to an energy of 14 eV from (2.8) we get an electron longitudinal temperature $T_{\parallel in}=4.4\cdot10^{-4}$ eV ($T_{\parallel in}/e^2 n_{in}^{1/3} \simeq 2.15$). From Fig. 19 we have the electron longitudinal temperature after an adiabatic accelepation up to an energy of 470 eV: $T_{\parallel fin}/e^2 n^{1/3} \simeq 0.27$ ($T_{\parallel fin}=3.1\cdot10^{-5}$ eV). A decrease in the electron density by the order of magnitude down to $n_e \simeq 5\cdot10^7$ cm^{-3} enables obtaining even a lower temperature value after an adiabatic acceleration: $T_{\parallel fin}/e^2 n^{1/3} \simeq 0.16$ ($W_{min}=3.0$ eV, $T_{\parallel in}/e^2 n^{1/3} \simeq 3.2$, $T_{\parallel fin}=8.5\cdot10^{-6}$ eV). Thus, a decrease in the electron current enables one to decrease the longitudinal temperature. The minimal value of temperature is achieved at a current value tending to zero and it is equal to $T_\parallel = T_c^2/2W \simeq 10^{-6}$ eV.

Electron beams with a temperature $T_\parallel \leqslant 10^{-2} e^2 n^{1/3}$ are of great interest. At such a low temperature in an electron beam an ordering appears i. e. the beams turn to be an «electron crystal». For obtaining such a cool electron beam an adiabatic acceleration up to a high energy is required. From Fig. 19 it follows that during an acceleration of an electron beam from the temperature $T_\parallel/e^2 n^{1/3} = 4$

to $T_\parallel/e^2 n^{1/3} = 10^{-2}$ the energy variation required is $\lg(W_{fin}/W_{in}) \simeq 5$. If an energy of accelerated electrons $W_{fin}=50$ keV an initial energy for the adiabatic acceleration should not be higher than $W_{in}=0.5$ eV, and an electron current not higher than 20 μA. From this evaluation it is evident that for obtaining the ordering the beam current should be very small. Within the current range used in the real experiments on electron cooling it is hard to attain such superlow temperatures $T_\parallel \leqslant 10^{-2} e^2 n^{1/3}$. The characteristic temperature value that can be obtained with the adiabatic acceleration is approximately by the order of magnitude lower than $e^2 n^{1/3}$ and it is in the limit $(0.5\div2)\cdot10^{-5}$ eV.

4.2. Maximal Decrements and Minimal Temperatures

As it was already mentioned a strong magnetic field accompanying an electron beam eliminates from the collision kinetics the transverse degree of freedom of the electron motion. In this case, an equilibrium temperature of the cooling beam of negatively charged ions is of the order of the longitudinal temperature of electrons, i. e. it can reach its very low values $T \leqslant 10^{-5}$ eV. In the case of positively charged ions an additional transverse diffusion (due to generation of bound electron-ion pairs) increase the transverse temperature. Although the ion longitudinal temperature can reach these minimal values. Thus, the use of an adiabatic acceleration of electrons in a gun enables one to achieve the temperature of a cooled beam by the order of magnitude lower than that obtained on the NAP-M installation which corresponds to the entirely ordered (longitudinally-crystallic) state in a cooled ion beam.

The use of the photocathode with a low temperature of emitted electrons does not give a quality in principle new from the viewpoint of obtaining the minimal temperature in the cooled ion beam, as at any other kind of emission the transverse degree of freedom of magnetized electrons is excluded from the cooling kinetics and the longitudinal temperature is mainly determined by the density of electrons and method of acceleration. From our point of view more essential is a possibility to decrease the electron transverse temperature which under the condition of magnetization will lead to a decrease in the internal scattering in an electron beam. This enables one together with the conservation of magnetization to increase the density of electrons on the cooling section without an increase in the magnetic field value (see (2.6), (2.7)).

The friction force maximum obtained in the experiments on the device «Model of Solenoid» is attained at the ion velocity noticeably higher than the longitudinal heat velocity of electrons. A further decrease in the electron longitudinal temperature cannot change substantially the friction force behaviour in the velocity range $v_p > \sqrt{e^2 n^{1/3}/m}$ an apparently cannot change the friction force maximum value. The friction force behaviour in the ion velocity range $v_p < \sqrt{e^2 n^{1/3}/m}$ at an ultimately low temperature of an electron beam $T \ll e^2 n^{1/3}$ needs an additional theoretical and experimental study.

CONCLUSION

In a strong magnetic field the electron transverse degree of freedom is magnetized and excluded from the kinetic of collisions. In this case, an electron effective temperature is determined by their longitudinal temperature and reaches very low values: the kinetic energy of electrons and potential energy of their collisions become of the same order of magnitude. At the same time, an efficiency of electron cooling is very sensitive to the conditions of generation and transportation of an electron beam. The theoretical calculations are very complicated here and the experiment acquires a decisive role.

The use of a strong magnetic field for accompanying an electron beam enabled to obtain the low effective temperature of electrons that led to a sharp increase in cooling efficiency in the range of low relative velocities. At the same time an essential difference was observed in cooling the positively and negatively charged ions.

The authors extend their sincere gratitude to V.G. Davidovsky, D.V. Pestrikov and V.D. Shiltsev for the useful discussions.

Appendix 1

The Friction Force Calculation for the Case of Ultimate Magnetization of Electron Motion with an Account of Collective Reaction of Electron Plasma

Let a heavy charged particle (ion) move through a plasma with a velocity $v_p \ll c$. In this case, a potential electric field is excited in the plasma and the plasma is characterized by the dielectric penetrability $\varepsilon_{k\omega}$ and for the harmonics of the electric field excited by an ion one can write down the following expression:

$$i(\mathbf{k}, \mathbf{E}_{k\omega}) = \frac{4\pi}{\varepsilon(k, \omega)} \rho_{k\omega}, \quad \mathbf{E}_{k\omega} = i\mathbf{k}\varphi_{k\omega} \tag{A1.1}$$

where

$$\rho_{k\omega} = \int e^{i(\omega t - \mathbf{k}, \mathbf{r})} e\delta(r - \mathbf{v}_p t)\, d^3r\, dt = 2\pi e\delta(\omega - k, \mathbf{v}_p) \tag{A1.2}$$

is the Fourier-harmonics of the charge density produced by the travelling ion. Performing the reverse Fourier-transformation and taking into account that one the electric field is a potential one, we get an electric field excited by an ion in a plasma:

$$\mathbf{E}(r, t) = \frac{e}{2\pi^2 i} \int \frac{\mathbf{k}}{k^2} \frac{d^3k d\omega}{\varepsilon_{k\omega}} e^{-i(\omega t - kr)} \delta(\omega - \mathbf{k}, \mathbf{v}_p). \tag{A1.3}$$

The friction force acting on the ion is determined correspondingly by the field with the subtruction of the ion eigen field:

$$\mathbf{F}_{fr} = e\mathbf{E}(\mathbf{v}t, t) = \frac{e^2}{2\pi^2 i} \int \frac{\mathbf{k}}{k^2} \left(\frac{1}{\varepsilon_{k\omega}} - 1 \right) d^3k \Big|_{\omega = (kv)} =$$

$$= \frac{e^2}{2\pi^2} \int \mathrm{Im} \left(\frac{1}{\varepsilon} \right) \frac{\mathbf{k}}{k^2} d^3k. \tag{A1.4}$$

As it is well known, the dielectric penetrability for an electron plasma is:

$$\varepsilon_{k\omega} = 1 - \frac{\omega_{pe}^2}{\omega^2} \frac{(\mathbf{k}, \hat{b})^2}{k^2} + \frac{i\delta}{\omega}, \tag{A1.5}$$

where $\hat{b}$ is a unit vector along the magnetic field, δ is a perturbation damping decrement: $0 < \delta \ll \omega_{pe}$; $\omega_{pe}^2 = 4\pi n e^2/m$ is a plasma frequency for electrons. Finally we get

$$F_{fr}=\frac{e^2}{2\pi^2}\int \mathrm{Im}\left[\frac{(k,v)^2 \mathbf{k}}{(\mathbf{k},\mathbf{v})^2k^2-\omega_{pe}^2(k,b)^2+i\delta k^2(\mathbf{k},\mathbf{v}_p)}\right]d^3k. \qquad (A1.6)$$

Further calculations are convenient to carry out in a cylindrical coordinate system with an exis directed along the particle velocity:

$$F_{fr}=\frac{e^2}{2\pi^2}\int \mathrm{Im}\left[\frac{k_{\parallel}^2\mathbf{k}}{k_{\parallel}^2(k_{\parallel}^2+k_{\perp}^2)-\frac{\omega_{pe}^2}{v_p^2}(k_{\perp}b_{\perp}\cos\varphi+k_{\parallel}b_{\parallel})^2+i\gamma|k_{\parallel}|}\right]k_{\perp}dk_{\perp}dk_{\parallel}d\varphi. \qquad (A1.7)$$

The calculating the integral over φ and tending $\gamma\equiv\frac{k^2\delta}{v_p}\to 0$ for the friction force components transverse and along the velocity we have:

$$\mathscr{F}_{\perp}=-\frac{e^2}{2\pi}\int\frac{k_{\perp}k_{\parallel}^2dk_{\perp}dk_{\parallel}}{\sqrt{k_{\perp}^2+k_{\parallel}^2}\,b_{\perp}\varkappa}\left[\frac{\sqrt{k_{\perp}^2+k_{\parallel}^2}-\varkappa b_{\parallel}}{\sqrt{\varkappa^2b_{\perp}^2k_{\perp}^2-k_{\perp}^2(\varkappa b_{\parallel}-\sqrt{k_{\perp}^2+k_{\parallel}^2})^2}}-\right.$$
$$\left.-\frac{\sqrt{k_{\perp}^2+k_{\parallel}^2}+\varkappa b_{\parallel}}{\sqrt{\varkappa^2b_{\perp}^2k_{\perp}^2-k_{\parallel}^2(\varkappa b_{\parallel}+\sqrt{k_{\perp}^2+k_{\parallel}^2})^2}}\right],$$
$$\mathscr{F}_{\parallel}=-\frac{e^2}{2\pi}\int\frac{k_{\parallel}^2k_{\perp}dk_{\parallel}dk_{\perp}}{\sqrt{k_{\perp}^2+k_{\parallel}^2}}\left[\frac{1}{\sqrt{\varkappa^2k_{\perp}^2b_{\perp}^2-k_{\parallel}^2(\varkappa b_{\parallel}-\sqrt{k_{\perp}^2+k_{\parallel}^2})^2}}+\right.$$
$$\left.+\frac{1}{\sqrt{\varkappa^2b_{\perp}^2k_{\perp}^2-(\varkappa b_{\parallel}+\sqrt{k_{\perp}^2+k_{\parallel}^2})^2}}\right]. \qquad (A1.8)$$

Here $\varkappa=\omega_{pe}/v_p$. Shifting to the polar coordinate system $k_{\perp}=k\sin\theta$, $k_{\parallel}=k\cos\theta$ and calculating the integral over for all θ, when the expression under the integral is real, we have:

$$\mathscr{F}_{\perp}=-\frac{e^2\varkappa b_{\perp}}{4}\int_0^{k_m}k^2dk\left\{\frac{k-\varkappa b_{\parallel}}{[\varkappa^2b_{\perp}^2+(k-\varkappa b_{\parallel})^2]^{3/2}}-\frac{k+\varkappa b_{\parallel}}{[\varkappa^2b_{\perp}^2+(k+\varkappa b_{\parallel})^2]^{3/2}}\right\},$$

$$\mathscr{F}_{\parallel}=-\frac{e^2}{4}\int_0^{k_m}k^2dk\left\{\frac{\varkappa^2b_{\perp}^2}{(\varkappa^2b_{\perp}^2+(k-\varkappa b_{\parallel})^2)^{3/2}}+\frac{\varkappa^2b_{\perp}^2}{(\varkappa^2b_{\perp}^2+(k+\varkappa b_{\parallel})^2)^{3/2}}\right\}. \qquad (A1.9)$$

It is taken into account that the integral is logarithmically divergent on the upper limit and the region of integration is limited by the value k_m. At $k_m\gg\varkappa$ the integrals are calculated easily. As a

result, within the logarithmic accuracy we get:

$$\mathscr{F}_{\perp}=-\frac{2\pi ne^4L_C}{mv^2}2b_{\perp}b_{\parallel},$$
$$\mathscr{F}_{\parallel}=-\frac{2\pi ne^4L_C}{mv^2}b_{\perp}^2. \qquad (A1.10)$$

Appendix 2

The Friction Force Calculation in the Case of Ultimate Magnetization of Electron Motion in Two-Particle Approximation

The calculation method is based on finding out the shift of each electron subjected to the action of the electric field of an incident particle and on further account of the reverse action of the electron on the incident ion. Since the Debye shielding is mainly a collective effect, in such a method of calculation in order to remove the divergencies at large impact parameters one should limit the interaction radius. Let us assume that an electric field of an incident particle is instantaneously «on» upon it reaches the Debye sphere with a radius r_D. Since the electron motion equation in the field of incident an ion is not integrated let us use the perturbation theory.

Let the ion move along the axis z so that its coordinates depend on time as $(x_p, y_p\ z_p)=(0, 0, v_pt)$, and the magnetic field vector is in a plane (x,z) and directed at an angle θ to the axes z, i. e. $\mathbf{B}=(B\sin\theta, 0, B\cos\theta)$. At $t=-\infty$ an electron is in rest and its coordinates are $(x_e\ y_e,\ z_e)=(\rho\cos\varphi, \rho\sin\ \varphi, 0)$, where ρ is an impact parameter of collisions. Under the influence of the electric field of an incident ion an electron shifts along the magnetic field by the value $\xi(t)$ according to the equation of motion:

$$\frac{d^2\xi}{dt^2}=\frac{e^2}{m}\frac{\rho\cos\varphi\sin\theta-v_pt\cos\theta}{(\rho^2+(vt)^2)^{3/2}}. \qquad (A2.1)$$

We take that an ion travels with a constant velocity v_p and a shift of the electron is small compared to the impact parameter of collisions. By integrating this equation we have:

$$\xi(z)=\frac{e^2}{mv_p^2}\int_{-z_0}^{z}dz_1\int_{-z_0}^{z_1}\frac{\rho\cos\varphi\sin\theta-z_2\cos\theta}{|\rho^2+z_2^2|^{3/2}}dz_2=$$

$$= \frac{e^2}{mv_p^2}\left[\frac{\sin\theta\cos\varphi}{\rho}\left(\sqrt{z^2+\rho^2}-\sqrt{z_0^2+\rho^2}+\frac{z_0(z+z_0)}{(z_0^2+\rho^2)^{1/2}}\right)-\right.$$

$$\left.-\cos\theta\left(\frac{z+z_0}{(z_0^2+\rho^2)^{1/2}}-\ln\frac{z+\sqrt{z^2+\rho^2}}{-z_0+\sqrt{z_0^2+\rho^2}}\right)\right]. \qquad (A2.2)$$

The momentum transfer from an electron to an ion is equal to:

$$\Delta p_i = e^2 \int_{-z_0/v_D}^{z_0/v_D} dt\, \xi_j \frac{\partial}{\partial r_j}\left(\frac{r_i}{r^3}\right) = \frac{e^2}{v_p}\int_{-z_0}^{z_0} \xi_j \frac{r^2\delta_{ij}-3r_ir_j}{r^5}\,dz, \qquad (A2.3)$$

where $\mathbf{r}=(\rho\cos\varphi,\ \rho\sin\varphi,\ -v_pt)$ is a distance between an electron and an incident ion. By integrating over the impact parameter we get the friction force

$$F_i = \int \Delta p_i \rho\, d\rho\, d\theta\, v = e^2 \int_{\rho_{min}}^{\rho_{max}} \rho\, d\rho \int_0^{2\pi} d\theta \int_{-z_0}^{z_0} \xi_j \frac{r^2\delta_{ij}-3r_ir_j}{r^5}\,dz. \qquad (A2.4)$$

From the condition of the interaction occurence at $r=r_D\equiv v_p/\omega_p$ it follows that

$$\rho_{max}=r_D, \quad z_0=\sqrt{r_D^2-\rho^2}.$$

The minimal impact parameter is determined by the condition of the perturbation theory applicability, i. e. a smallness of a shift with respec to the impact parameter. From (A2.2) we get

$$\xi(0)=\frac{e^2}{mv_p^2}\left[\sin\theta\cos\varphi-\cos\theta\left(1-\ln\frac{2r_D}{\rho}\right)\right], \quad r_D\gg\rho, \qquad (A2.5)$$

whence

$$\rho_{min}\simeq\frac{e^2}{mv_p^2}\ln\frac{2r_D}{\rho_{min}}\simeq\frac{e^2}{mv_p^2}\ln\left(\frac{r_Dmv_p^2}{e^2}\right). \qquad (A2.6)$$

Substituting (A2.2) into (A2.4) an performing integration in a logarithmic approximation we get the friction force components along and transverse to the ion velocity:

$$\mathcal{F}_{\parallel}=-\frac{2\pi ne^4L_C}{mv_p^2}\sin^2\theta, \quad L_c\simeq\ln\frac{r_D}{r_{min}},$$

$$\mathcal{F}_{\perp}=-\frac{2\pi ne^4L_C}{mv_p^2}\cos\theta\sin\theta. \qquad (A2.7$$

In the expression obtained the friction force components are twic lower than in (A1.10). The difference is connected with the fact tha in the calculation given the contribution of small impact distance was neglected.

REFERÈNCES

1. *Budker G.I.* Effective Method for Damping Particle Oscillations in the Protoı and Antiproton Storage Rings. Atomnaya Energia, 1967, v.22, N 5, p.246—248.
2. *Budker G.I., Skrinsky A.N.* Electron Cooling and New Possibilities in Physics o Elementary Particles.—UFN, 1978, v.124, N 4, p.561.
3. *Budker G.I., Bulushev A.F., Dykansky N.S. et al.* New Results in a Study o Electron Cooling. Proceedings of V All-Union Meeting on Accelerators o Charged Particles. M.: Nauka, 1977, v.1, p.236—239.
4. *Derbenev Ya.S., Skrinsky A.N.* Magnetization Effects in Electron Cooling —Plasma Physics, 1978, v.4, N 3, p.492—500.
5. *Dikansky N.S., Kononov V.I., Kudelainen V.I. et al.* A Study of Fast Electror Cooling.—Proceedins of VI All-Union Meeting on Charged Particle Accelerators Dubna, 1979, v.1, p.99—106; Preprint INP 79-56. Novosibirsk, 1979.
6. *Skrinsky A.N., Parkhomchuk V.V.* Methods for Cooling Beams of Charged Particles—EChAYa, 1981, v.12, issue.3, p.557—613.
7. *Bell M. et al.* Electron Cooling in ICE at CERN.—Nucl. Instr. and Meth., 1981, v.190, N 2, p.235—255.
8. *Foster R. et al.* Electron Cooling Experiments at Fermilab.—IEEE Trans. Nucl. Science, 1981, v.NS-28, N 3, p.2386—2388.
   Ellison T. et al. Electron Cooling and Accumulation of 200 MeV Protons at Fermilab.—IEEE Trans. Nucl. Science, 1983, v.NS-30, N 4, p.2370—2372.
9. *Dikansky N.S., Kokoulin V.I., Kot N.H. et al.* Fast Electron Cooling in the Range of Low Relative Velocities.—Proceedings of XIII Intern. Conf. on Accelerators of High Energy. Novosibirsk: Nauka, 1987, v.1, p.330—333.
10. *Dikansky N.S., Kot N.H., Kudelainen V.I. et al.* An Influence of The Ion Charge Sign on Friction Force during Electron Cooling—Preprint INP 87-102. Novosibirsk, 1987.
11. *Parkhomchuk V.V.* Physics of Fast Electron Cooling.— Proc. of Workshop on Electron Cooling and Related Applications, 1984, Karlsruhe.
12. *Kudelainen V.I., Lebedev V.A., Meshkov I.N., Parkhomchuk V.V., Sukhina B.N.* Temperature Relaxation in Magnetized Electron Flux.—JETP, 1982, v.83, issue 6(12), p.2056—2064.
13. *Sery A.A.* Electron Cooling of Velocity Small Spread: Diploma Thesis, Novosibirsk State University, Novosibirsk, 1986.
14. *Piwinski A.* IX Intern. Conf. on High Energy Accelerators.—Stanford, California, May 1974, p.405.
15. *Kot N.H., Sukhina B.N.* Experience in Explotation and Development of Electrostatic Accelerator EG-1.5 and GEVW 0.5/2000.—Voprosy Atomnoi Nauki i Tekhniki. Technics of Physical Experiment, 1985, issue 1(22), p.7—9.

16. *Kot N.H., Lebedev V.A., Ovchar V.K., Ostanin V.P., Parkhomchuk V.V., Sukhina B.N.* Computer Control of Parameters and Equipment Located inside the High Voltage Electrode of Injector EG-1.5.—Voprosy Atomnoi Nauki i Techniki, Technics of Physical Experiment, 1985, issue 1(22), p.59—61.
17. *Kot N.H., Parkhomchuk V.V.* A Three-Beam Source of Hydrogen Negative Ions on Water Vapour—Pribory i Tekhnika Experimenta, 1985, issue 1(22), p.59—61.
18. *Lebedev V.A., Sharapa A.N.* Formation of Electron Beam with Small Transverse Velocities in Systems with Longitudinal Magnetic Field.—JTF, 1987, v.57, N 5, p.975.
19. *Arapov L.N., Dykansky N.S., Kokoulin V.I., Kudelainen V.I., Lebedev V.A., Parkhomchuk V.V., Smirnov B.N., Sukhina B.N.* Precision Solenoid for Electron Cooling.—Proceedings of XIII Intern. Conf. on High Energy Particle Accelerators. Novosibirsk: 1987, v.1, p.341—343.
20. *Dementiev E.I., Dikansky N.S., Medvedko A.S. et al.* Measurement of Heat Noise of Proton Beam on the Storage Ring NAP-M.—JTF, 1980, v.50, N 8, p.1717—1729.
21. *Parkhomchuk V.V., Pestrikov D.V.* Heat Nose of Intense Beam in Storage Ring.—JTF, 1980, v.50, N 7, p.1411—1418.
22. *Dikansky N.S., Pestrikov D.V.* Influence of Ordering Effects on Relaxation of Nonbunched Cool Beam in Storage Ring.—JTF, 1986, issue. 2, p.289—296; issue.3, p.505—514.
23. *Feigerle C.S., Pierce D.T., Seiler A., Celotta R.J.* Appl. Phys. Lett, 1986, v.44, p.866.
24. *Landau L.D. Livshits E.M.* Statistical Physics, v.V, part 1.—M.: Наука, 1976.
25. *Parkhomchuk V.V.* Physics of Fast Electron Cooling.—Doctoral Thesis. Novosibirsk, INP, 1985.
26. *Kiselev A.B., Nikonov B.P., Tursunmetov K.A.* Radiotechnika i Electronika, 1975, v.20, p.1041.

N.S. Dikansky, V.I. Kudelainen, V.A. Lebedev, I.N. Meshkov, V.V. Parkhomchuk, A.A. Sery, A.N. Skrinsky, B.N. Sukhina

Ultimate Possibilities of Electron Cooling

Н.С. Диканский, В.И. Куделайнен, В.А. Лебедев, И.Н. Мешков, В.В. Пархомчук, А.А. Серый, А.Н. Скринский, Б.Н. Сухина

Предельные возможности электронного охлаждения

Ответственный за выпуск С.Г.Попов

Работа поступила 20 апреля 1988 г.
Подписано в печать 5.05. 1988 г. МН 08305
Формат бумаги 60×90 1/16 Объем 3,7 печ.л., 3,0 уч.-изд.л.
Тираж 290 экз. Бесплатно. Заказ № 107

Набрано в автоматизированной системе на базе фотонаборного автомата ФА1000 и ЭВМ «Электроника» и отпечатано на ротапринте Института ядерной физики СО АН СССР,
Новосибирск, 630090, пр. академика Лаврентьева, 11.